TITLE: Branching Varies with Light Limitation Scenarios in relation with Changes in Carbon Source-Sink Dynamics

SHORT TITLE: Branching regulation by Light and Source-Sink balance

Anne Schneider[1], Frédéric Boudon[2,3], Sabine Demotes-Mainard[1], Lydie Ledroit[1], Maria-Dolores Perez-Garcia[1], Cédric Cassan[4], Yves Gibon[4], Christophe Godin[5], Soulaiman Sakr[1], Jessica Bertheloot[1,6*]

[1]Univ Angers, Institut Agro, INRAE, IRHS, SFR QUASAV, F-49000 Angers, France
[2]CIRAD, UMR AGAP Institut, 34398 Montpellier, France
[3]AGAP Institut, CIRAD, INRAE, Institut Agro, Université de Montpellier, Montpellier, France
[4]INRAE, Univ. Bordeaux, UMR 1332, Biologie du Fruit et Pathologie, 33882 Villenave d'Ornon, France
[5]Laboratoire Reproduction et Developpement des Plantes, University of Lyon, ENS de Lyon, UCB Lyon 1, CNRS, INRA, Inria, F-69342, Lyon, France
[6]LEPSE, Univ Montpellier, INRAE, Institut Agro Montpellier, Montpellier, France

*Correspondence : jessica.bertheloot@inrae.fr

Anne Schneider anneschneider@hotmail.fr
Frederic Boudon frederic.boudon@cirad.fr
Sabine Demotes-Mainard sabine.demotes-mainard@inrae.fr
Lydie Ledroit lydie.ledroit@agrocampus-ouest.fr
Maria Dolores PEREZ-GARCIA maria-dolores.perez-garcia@agrocampus-ouest.fr
Cédric Cassan cedric.cassan@inrae.fr
Yves Gibon yves.gibon@inrae.fr
Christophe Godin christophe.godin@inria.fr
Soulaiman SAKR soulaiman.sakr@agrocampus-ouest.fr
Jessica Bertheloot jessica.bertheloot@inrae.fr

Date of submission : 2026/01/27

Word count : 5874

Supplementary data : 15 supplementary figures

Highlight

Bud outgrowth, a key component of plant plasticity, is regulated by light intensity through sugar availability. Continuous and transient low light have opposite effects by limiting sugar production and use, respectively.

Abstract

Bud outgrowth is a major component of plant architectural plasticity and is influenced by light conditions. While the inhibitory effect of low light intensity on branching is well documented, the underlying regulators remain debated and, especially, the role of sugar availability has never been thoroughly evaluated. Here, we combined experiments with a computational approach quantifying carbon source-sink balance in single-axis rose plants to investigate how continuous and transient light limitation regulate bud outgrowth. Continuous low light reduced photosynthesis, leading to decreased sugar availability and inhibited bud outgrowth. In contrast, a transient period of low light followed by high light unexpectedly stimulated bud outgrowth, shortened the delay between outgrowth of successive buds, and produced an over-branched phenotype. This response resulted from a non-reversible reduction in the growth of apical organs appearing under low light, which lowered carbon demand and caused sugar over-accumulation after the return to high light. Manipulating carbon supply and demand through leaf masking, photosynthetic inhibition, and targeted sucrose feeding causally confirmed the central role of sugar availability in these contrasting responses. Beyond these findings, key requirements for models simulating branching plasticity were identified and this work provides a basis for predicting branching responses under fluctuating and complex light environments.

Keywords: Architecture, Branching, Bud outgrowth, Light, Modelling, Plasticity, Source-Sink, Sugar

Introduction

As sessile organisms, plants exhibit high developmental plasticity, enabling them to adapt to their environment. Axillary bud outgrowth is a major component of this plasticity: buds are initiated at each leaf axil and may either grow immediately or enter dormancy that is released when conditions become favorable, thereby generating new axes and enabling space colonization (Barthelemy and Caraglio, 2007; Lang *et al.*, 1987). This response strongly affects agronomic performance (yield, visual quality in ornemental plants; Borrell *et al.*, 2014; Boumaza *et al.*, 2010; Crespel *et al.*, 2020; Slafer *et al.*, 2014) and therefore must be finely tuned to growing conditions. Light in particular is a major regulator of branching and can vary strongly due to climatic fluctuations (cloudy periods) or artificial lighting in indoor production systems (Noia *et al.*, 2023; SharathKumar *et al.*, 2020). While several studies have investigated light quality (Demotes-Mainard *et al.*, 2016), the impact of light quantity on bud outgrowth has received less attention. Most studies indicate that low light quantity represses branching (Corot *et al.*, 2017; Demotes-Mainard *et al.*, 2013b; Leduc *et al.*, 2014; Mitchell, 1953a; Su *et al.*, 2011), although transient low-light periods can stimulate branching (Demotes-Mainard *et al.*, 2013b; Lafarge *et al.*, 2010), highlighting the complexity of this response. The underlying physiological mechanisms remain debated (Schneider *et al.*, 2019).

Historically, research has focused on apical dominance, the phenomenon by which growing apical organs inhibit the buds located below (Cline, 1991; Thimann and Skoog, 1933). Auxin, produced by apical organs and transported basipetally, inhibits bud outgrowth through interactions with cytokinins (CK) and strigolactones (SL) (Domagalska and Leyser, 2011; Schneider *et al.*, 2019). However, growing evidence over the last decade has highlighted a major role of low sugar availability for buds, due to the strong sink activity of apical organs. A pioneering study in pea (Mason *et al.*, 2014) showed that, following decapitation, basal bud release preceded any detectable decrease in auxin in adjacent stem tissues, whereas an increase in sugar levels was observed. The causal link between increased sugar availability and bud release was demonstrated by exogenous sugar supply in plants with intact apices, which promoted bud outgrowth.

Additional support for a key role of sugar availability comes from experiments manipulating sugar supply or demand for growth in various species. Partial defoliation reduced bud growth in sorghum (Kebrom and Mullet, 2015), while *tin* wheat mutants with earlier stem growth exhibited reduced branching (Kebrom *et al.*, 2012). *In vitro* studies using isolated stem segments further demonstrated that increasing sugar concentration in the medium promotes bud outgrowth dose-dependently by enhancing both its frequency and the time at which bud outgrowth start (Barbier *et al.*, 2015b; Henry *et al.*, 2011; rose). For rose, experiments using non-metabolizable sucrose analogs showed that sucrose partly acts as a signalling molecule, interacting with hormonal pathways (Barbier *et al.*, 2015b; Bertheloot *et al.*, 2020; Rabot *et al.*, 2012). Consistently, in pea, the level of trehalose-6-phosphate (T6P) in the bud, a proxy for sucrose availability, strongly correlated with bud outgrowth triggered by plant decapitation or exogenous sucrose supply *in vitro* (Fichtner *et al.*, 2017). Increased sugar availability rapidly activates bud metabolism, making the bud an active sink for sugars (Henry *et al.*, 2011; Wang *et al.*, 2022; Wang *et al.*, 2021).

Because light intensity strongly modulates photosynthesis and sugar production (e.g., Hirose and Werger, 1987), it has been hypothesized that light limitation inhibits bud outgrowth by reducing sugar supply, thereby reinforcing apical dominance. This view is indirectly supported by studies showing that the promoting effect of light on grass tillering is reduced at higher temperatures, which enhances organ growth and sugar consumption (Bos and Neuteboom, 1998; Mitchell, 1953b). More quantitative studies also reported correlations between tillering level and indices integrating radiation, leaf size and

expansion rate at the critical period for tiller appearance (Alam *et al.*, 2014; Alam *et al.*, 2017; Kim *et al.*, 2010). Accordingly, several ecophysiological models implement branching control via a competition index reflecting the balance between carbohydrate (C) production by source organs and C use by sinks for growth (Evers *et al.*, 2010; Luquet *et al.*, 2006; Mathieu *et al.*, 2009; Warren-Wilson, 1972). While such index has been shown to reproduce sugar reserves dynamics under a specific condition, supporting that it is a good proxy for sugar availability, direct physiological evidence that sugar availability drives branching response to light is lacking.

In rose, sugar availability does not appear to be the limiting factor for bud outgrowth inhibition under low light, despite reduced stem sugar concentrations (Corot *et al.*, 2017; Roman *et al.*, 2016b). Exogenous sugar supply failed to stimulate bud outgrowth under low light, both in intact plants and in decapitated and defoliated plants kept in darkness. In contrast, exogenous application of CK, that displayed reduced levels under low light, restored bud outgrowth, indicating that CK rather than sugars are limiting. Similarly, increased tillering in wheat was observed in response to higher day-time light intensity, regardless of sugar concentration (Lorenzo *et al.*, 2015). These results call for a reassessment of the role of sugars in the light intensity-mediated bud outgrowth.

Furthermore, the concept that light intensity primarily promotes bud outgrowth by increasing photosynthesis and carbohydrate supply needs to be reexamined, given that light also induces morphological and physiological adaptations that may counterbalance its effect on photosynthesis. Low light tends to stimulate organ elongation (e.g. internodes and leaves), enhancing light interception (Chenu *et al.*, 2005; Dong, 1995; Garcia-Martinez and Gil, 2001; Hitz *et al.*, 2019; Jiang *et al.*, 2021), which may partially compensate for reduced light availability. Leaf appearance rate and expansion have also been reported to decrease (Baumont *et al.*, 2019; Chenu *et al.*, 2005; Gautier *et al.*, 1999; Milthorpe and Newton, 1963), thereby reducing sink demand. Conversely, the photosynthetic apparatus acclimates to low light, decreasing photosynthetic capacity which may strengthen the impact of low light (Grindlay, 1997; Sims and Pearcy, 1992). Together, this highlights the need for a quantitative approach—currently lacking—to analyze how light intensity affects carbohydrate availability and bud outgrowth. Such an approach must also be dynamic, given the reported irreversible effects of transient low light on plant development and physiology (Granier and Tardieu, 1999a; Sims and Pearcy, 1992).

The objective of this study is therefore to re-evaluate the prevailing view that branching responses to light intensity primarily result from changes in sugar availability within the plant, using rose as model species. We investigated the effects of both continuous and transient light limitation, the latter leading to a counter-intuitive stimulation of branching (Demotes-Mainard *et al.*, 2013b). Beside measuring bud outgrowth and sugar levels, our approach integrates detailed measurements of plant development and photosynthetic capacity into a computational model to dynamically quantify source-sink balance. Complemented by targeted source-sink manipulations, this integrative framework allows us to disentangle and explain the relationships between light intensity, sugar availability, and bud outgrowth.

Material and methods

Plant material, growth conditions, and light treatments

Single-node cuttings of *R. hybrida* 'Radrazz' plants were obtained as described in Demotes-Mainard et al. (2013). They were grown in 500 ml pots containing a 50/40/10 mixture of neutral peat, coconut

fibers and perlite in a temperature-controlled greenhouse till 3 leaves were visible, and were kept disease-free. Then plants were transferred to a growth chamber (light/dark 16/8h photoperiod; 22/20°C day/night temperature; air humidity 60-70%) until the flower of the primary axis faded. Plants were sub-irrigated every two or three days with a fertilized solution (5.0 mM KNO3, 2.0 mM Ca(NO3)2, 2.0 mM NH4NO3, 2.0 mM KH2PO4, 2.0 mM MgSO4, 0.25 mM NaOH) and additional trace elements: Kanieltra formula 6-Fe at 0.25 $ml.l^{-1}$ (Hydro Azote, Nanterre, France) to maintain optimal hydric and mineral nutrition.

In growth chambers, plants were submitted to three different light intensity regimes described in Fig. 1: a constant low light intensity (LL), a constant high light intensity (HH), or a transient light limitation until the floral bud becomes visible at the top of the primary axis (FBV stage; LH) followed by a return to high light intensity. A first experiment (Exp. 1) was made in 2011 in two identical growth chambers (Froids et Mesures, Beaucouzé, France), with a photosynthetic flux density (PPFD) of *ca.* 420 µmol m^{-2} s^{-1} at plant height (60 cm above the culture table) for high light, and *ca.* 90 µmol m^{-2} s^{-1} for low light. Plants were grown in 6 rows (including two border rows) with one plant every 15 cm. Since different growth chambers were used for the different light treatments, temperature was recorded, and time was expressed in degree days (2.1°C as base temperature; see Demotes-Mainard et al., 2013) to account for temperature differences between growth chambers. Other experiments (Exp. 2-3-4, 2018-2021) were made in a unique Strader growth chamber, with PPFD of *ca.* 80 µmol m^{-2} s^{-1} for low light and *ca.* 310 µmol m^{-2} s^{-1} for high light. Plants were grown in 2 rows with, similarly to Exp. 1, one plant every 15 cm. Since light treatments were applied concomitantly in the same growth chamber under a similar temperature, time was expressed in days and not degree days.

Plant architectural description

Studied rose plants are composed of primary axes that develop from the initial cutting (see Fig. 1). Each primary axis consists of a succession of vegetative phytomers, topped by a peduncle, that appear successively till the floral bud becomes visible at the top (FBV stage). Each phytomer consists of an internode, a leaf at the top, and an axillary bud at leaf axil, except for the most basal phytomers that are unleafy (called “basal part”). From the axillary buds, secondary axes develop after FBV stage. Each leafy phytomer of the primary axis was numbered from plant base, *n* being the total number of phytomers and *n*+1 being the peduncle. Phytomers were allocated to a zone, Z1, Z2, or Z3 (Fig. 2B; Fig. S2) according to their relative rank *r* (Z1: $0.7 \leq r \leq 1$; Z2: $0.4 \leq r < 0.7$; Z3: $0 \leq r < 0.4$):

$$r = \frac{i-1}{n-1} \quad for \;\; i <= n$$
$$r = 1 + \frac{1}{n} \quad for \;\; i = n+1 \qquad (5)$$

where *i* is the leafy phytomer number.

Dynamic quantification of plant architectural development and growth (Exp. 1)

For Exp. 1, the rose canopy in each light treatment was divided in two groups: one group of 12 plants for non-destructive measurements, and one group of 24 plants for destructive measurements. For each primary axis of each group, the date at which the plant emerged on the cutting (bud outgrowth) and the floral stages (Fig. 1; FBV, floral visible stage; PCV, petal color visible; OF, opened flower; FF, faded flower) were recorded every one or two days.

In the first group, the number of visible leaves on each primary axis was counted every 1 or 2 days except for LH, which was assumed to follow a similar pattern compared to LL since leaves appear before FBV, so under the same PPFD for LL and LH. Leaf appearance date was estimated assuming a

186 linear correlation between leaf relative rank and thermal time, as done earlier (Demotes-Mainard *et*
187 *al.*, 2013a). In addition, the development stage (dormant or outgrowing) of each axillary bud along
188 primary axes was scored from FBV stage every 2 days. An axillary bud was considered to start its
189 outgrowth when its first leaf was clearly visible between its scales.

190 In the second group, several sub-group of 4 to 5 plants were identified for harvesting at (i) FBV, just
191 after plant transfer to high light for LH, (ii) *ca.* 130°Cd after FBV, and (iii) at or after the end of organ
192 expansion. In the morning, each plant was separated into its root compartment, the primary axis basal
193 part, each internode+node, each leaf, the peduncle, the floral organ, and each axillary branch. Then,
194 each organ or compartment was immediately scanned (except roots and secondary branches),
195 transferred in frozen nitrogen, stored at -80°C, lyophilized, and weighted. From scans, the area of each
196 fully-opened leaf, the length of the terminal leaflet of each leaf, as well as the length and diameter of
197 each internode was determined using ImageJ (https://imagej.nih.gov/ij/).

198 **Quantification of sugar contents (Exp. 1-2)**

199 Samples of roots and primary axis individual organs or compartments of Exp. 1 were lyophilized then
200 ground, and aliquots of 10 mg fractionated with H_2O/EtOH as in Cross *et al.* (2006). Proteins were
201 extracted by adding 400 µl NaOH 0.1 M to the pellet, vigorous shaking and heating at 95 °C for 30 min.
202 After centrifugation at 2,000 g for 10 min, protein content was measured as in Bradford (1976). After
203 neutralization with HCl 0.5 M, starch was digested and quantified in the the resuspended pellet as in
204 Hendriks *et al.* (2003). Glucose, fructose and sucrose were measured in the supernatant as in Stitt *et*
205 *al.* (1989), nitrate as in Tschoep *et al.* (2009) and total amino acids as in Bantan-Polak *et al.* (2001). All
206 liquid handling steps were performed with Star and Starlet pipetting robots (Hamilton, Villebon sur
207 Yvette, France). Extractions were performed in 1.1 ml Micronic tubes (Lelystad, The Netherlands) and
208 all assays in polystyrene 96-well flat-bottom microplates. Absorbances were read at 600 (protein), 340
209 (starch and soluble sugars) and 540 (nitrate) nm in MP96 microplate readers (SAFAS, Monaco).
210 Fluorescence (amino acids, 405 nm excitation, 485 nm emission) was measured in a Xenius fluorimeter
211 (SAFAS, Monaco).

212 In addition, a complementary experiment, Exp. 2, was undertaken with the aim to specifically quantify
213 metabolites in the primary axis before bud outgrowth period. Plants were grown in the same growth
214 chamber under HH, LH, or LL, and four groups of at least four plants were pooled at (i) FBV, just before
215 plant transfer to high light for LH, (ii) 4 days after FBV for HH and LH, and (iii) 7 days after FBV for HH,
216 LH, LL. In each group, leaves and nodes (segments with 5 mm of stem each side of the node) of each
217 zone of primary axes were separated and immediately frozen in liquid nitrogen and stored at -80°C in
218 the morning. Samples were then lyophilized, ground, and soluble sugars (sucrose, glucose, fructose),
219 starch, nitrate, total amino-acids, and soluble proteins and starch were quantified with the same
220 method as in Exp. 1. In addition, total polyphenols were measured in the supernatant as in Colombié
221 *et al.* (2023). In parallel, bud outgrowth was quantified as for Exp. 1, every 2 days from FBV, on a subset
222 of 15-20 plants.

223 ***In vitro* culture of isolated stem segments**

224 To test if an increase in sugar availability for buds is correlated to an increase in stem sucrose and
225 starch contents (Fig. S4), a stem segment with one bud was excised from 10 rose primary axes at FBV
226 stage, and grown two days on a medium supplemented with either mannitol (100 mM) or sucrose at
227 different concentrations (10, 50, 100, 250 mM), as described previously (Barbier *et al.*, 2015b). 48h
228 after transfer on the culture medium, stem segments were collected in liquid nitrogen, and sugar
229 content analyses were performed on three independent biological samples using 50 mg of frozen
230 tissues per sample, similarly to Bertheloot *et al.* (2020).

Quantification of photosynthesis variables and final dimensions of primary axis organs (Exp. 3)

Fourteen to seventeen plants were grown under HH, LH, or LL, and for each plant, the date at which the plant emerged on the cutting and the number of visible leaves were recorded each day. When the fourth leaf was visible, 3 times per week, the length of the terminal leaflet of each leaf was measured, the floral stage of the primary axis recorded, and the chlorophyll index of each leaflet measured using Dualex device (Dualex 4 Scientific, Cerovic *et al.*, 2012) till OF stage. Chlorophyll index of each leaf was calculated as the mean of the measurements per leaflet. In addition, net photosynthesis was measured on a subset of 5 plants at 3-4 days after FBV for the terminal leaflet of leaves at ranks 1 and 4, at 100 and 600 µmol m^{-2} s^{-1} PPFD, using LICOR device (LI-6400 XT, LI-COR, Lincoln, NE, United States; 10/90% blue/red light, 400 µmol CO_2, 70% relative humidity, 22°C for temperature). On another subset of 10 plants, PPFD at each leaf level was measured at 3, 10 and 14 days after FBV using a quantum sensor (LI-190R Quantum Sensor, LI-COR, Lincoln, NE, United States) placed near the terminal leaflet and pointing upward.

At OF stage -once primary axes had finished their development-, each leaf and internode of each plant under HH and LH was separated similarly to Exp. 1, scanned, and leaf areas, terminal leaflet lengths, and internodes/peduncle lengths and diameters were determined using ImageJ (https://imagej.nih.gov/ij/).

Estimation of plant C availability

C availability I_c was estimated at each time step *t* (°Cd) for a primary axis of a rose plant grown in Exp. 1 under HH, LH, or LL, from FBV stage till *ca.* 300 °Cd after FBV (period of sugar accumulation for all treatments).

I_c <u>calculation model</u>

I_c (dimensionless) was calculated as the ratio between C supply (mg C °Cd^{-1}) by photosynthesis and C demand (mg C °Cd^{-1}), defined as C needed to build the structure of plant organs (Luquet *et al.*, 2006; Tabourel-Tayot and Gastal, 1998):

$$I_C(t) = \frac{Supply(t)}{Demand(t)} \qquad (2)$$

In this way, an I_c above 1 indicates an excess in C while an I_c below 1 indicates a C shortage.

Both the supply and demand were dependent on the temporal expansion dynamics of plant organs. The increases in leaf *i* area, $A_{i,lf}$ (cm^2), and internode *i* length, $L_{i,in}$ (cm), including the peduncle, were described by logistic functions of time saturating at maxima $A_{i,lf}^{max}$ (cm^2) and $L_{i,in}^{max}$ (cm) respectively, with normalized maximum rates, w_{lf} and w_{in} (°Cd^{-1}), at $t_{i,lf}^{*}$ and $t_{i,in}^{*}$ (°Cd), respectively (Demotes-Mainard *et al.*, 2013a):

$$A_{i,lf}(t) = \frac{A_{i,lf}^{max}}{1 + \exp(4 \cdot w_{lf} \cdot (t_{i,lf}^{*} - t))} \qquad (3)$$

$$L_{i,in}(t) = \frac{L_{i,in}^{max}}{1 + \exp(4 \cdot w_{in} \cdot (t_{i,in}^{*} - t))} \qquad (4)$$

The supply was the sum of each leaf *i* photosynthesis, calculated as the product of leaf *i* area and surfacic photosynthesis, $P_{i,lf}$ (µmol C m^{-2} s^{-1}), that was estimated as a rectangular hyperbolar of intercepted PPFD (Equatiion 9), $PPFD_{i,lf}$ (µmol photons m^{-2} s^{-1}) (Thornley, 1998):

$$\begin{aligned} Supply(t) &= c \times \sum_i \left(A_{i,lf}(t) \times 10^{-4} \times P_{i,lf}(t)\right) \\ &= c \times \sum_i \left(A_{i,lf}(t) \times 10^{-4} \times \left(\frac{\alpha \times PPFD_{i,lf}(t) \times p_{i,lf}^{max}(t)}{\alpha \times PPFD_{i,lf}(t) + p_{i,lf}^{max}(t)} - R\right)\right) \end{aligned} \quad (5)$$

where *c* is a conversion coefficient (mg C µmol C^{-1} s °Cd^{-1}), R is the respiration (assumed constant, µmol m^{-2} s^{-1}), α the photosynthetic efficiency (mol C . mol photons^{-1}), and $p_{i,lf}^{max}$ (µmol C m^{-2} s^{-1}) the maximum photosynthesis at saturating PPFD level depending on leaf rank and its development stage as detailed below.

C demand is the C used at each time step to build the structure of plant organs:

$$Demand(t) = \sum_{i,org} \left(\frac{\mathrm{d}C_{i,org}^{struct}(t)}{\mathrm{d}t}\right) \quad (6)$$

with $C_{i,org}^{struct}$ being the C involved in organ (*org*) *i* structure, organ being the leaves, the internodes, the basal part, the flower of the primary axis, as well as roots and secondary axes.

For the leaves and internodes, the C demand was decomposed as C used for the increase in dimensions (leaf area, internode volume expressed as a function of length and diameter $D_{i,in}$ (cm)) and for the increase in thickness (structural C mass per unit area, $CA_{i,lf}$ (mg C cm^{-2}), for leaves, and unit volume, $CV_{i,in}$ (mg C cm^{-3}), for internodes).
For the leaves, the C demand is thus:

$$\frac{\mathrm{d}C_{i,lf}^{struct}(t)}{\mathrm{d}t} = \frac{\mathrm{d}\left(A_{i,lf}(t) \times CA_{i,lf}(t)\right)}{\mathrm{d}t} \quad (7)$$

And for the internodes, it is formalized as:

$$\frac{\mathrm{d}C_{i,in}^{struct}(t)}{\mathrm{d}t} = \frac{\left(\mathrm{d}L_{i,in}(t) \times (\frac{D_{i,in}(t)}{2})^2 \times \pi \times CV_{i,in}(t)\right)}{\mathrm{d}t} \quad (8)$$

I_c estimation

From measurements of leaf appearance, final organ dimensions, photosynthesis, chlorophyll index, and organ dry masses, I_c was estimated each 10°Cd for median plants that were grown under HH, LH, or LL in Exp. 1 using equations above. The primary axis of these median plants was made of 8 leafy phytomers for LL and LH, and 9 for HH (Fig. S6). In measurements, axes may have a different number of phytomers compared to the median plant in each treatment. Estimations were made after attributing to each measured organ at rank *i* a median plant-equivalent rank, calculated from the actual relative rank and the targeted median number of phytomers, according to equation 1.

Estimations of leaf and internode expansions (Equations 3-4). On the one hand, inflexion dates of individual leaves and internodes, $t_{i,lf}^*$ and $t_{i,in}^*$ respectively, were estimated as pre-established polynomial functions of measured leaf appearance dates for each individual plant in Exp. 1 (Demotes-Mainard *et al.*, 2013a). Then, a cubic smooth spline was adjusted on inflexion dates as a function of

the relative rank, for HH and LL, giving access to the average inflexion dates for individual leaves and internodes of a median primary axis in HH and LL (Fig. S9A). Estimated inflexion dates of LL were used for LH, since LL and LH organs appeared under similar low light intensity. On the other hand, maximum areas of individual leaves $A_{i,lf}^{max}$ and maximum lengths of individual internodes $L_{i,in}^{max}$ were estimated as means of areas and lengths, respectively, per median plant-equivalent rank (Fig. S9B). After statistical analysis on measured data, similar values were set up for leaf areas for LH and HH for ranks ≤ 5 as well as LL and HH for rank > 5. For internodes, similar values were set up for all treatments for ranks ≤ 5. Finally, by integrating estimated inflexion point dates and final dimensions in equations 3-4, w_{lf} and w_{in} were manually adjusted so that estimated leaf and internode expansion dynamics, $A_{i,lf}$ and $L_{i,in}$, fitted the measured ones (Fig. S10-11).

Supply estimation (Equation 5).

In Exp. 1, $PPFD_{i,lf}$ was approximated as a function of cumulative leaf area index (LAI , leaf area per unit soil area) above leaf *i* and incident PFFD ($PPFD_0$), using the Beer-Lambert's law:

$$PPFD_{i,lf}(t) = PPFD_0 \times \exp\left(-k \times LAI(t)\right) \qquad (9)$$

where *k* is the light extinction coefficient. *k* was estimated using Exp. 3 data of PPFD (Fig. S7) and corresponding estimated leaf areas. Leaf expansions were estimated with the methodology described for Exp. 1 from measured leaf appearance dates and maximum areas (data not shown).

To estimate the surfacic photosynthesis $P_{i,lf}$ response to $PPFD_{i,lf}$, the parameters of the photosynthesis response curve to PPFD, α and $p_{i,lf}^{max}$, were first estimated on Exp. 3 data by fitting (Equation 5) to photosynthesis measured for ranks 1 and 4 at 100 and 600 µmol m^{-2} s^{-1} PPFD (Fig. 4A). Then, a linear dependence of $p_{i,lf}^{max}$ with leaf N status (Bertheloot *et al.*, 2011; Grindlay, 1997) depending on leaf age and rank, was introduced using leaf chlorophyll index, $chl_{i,lf}$, as a proxy for leaf N status (Bertheloot *et al.*, 2011). Temporal dynamics were estimated from Exp. 3 chlorophyll measurements after statistical analysis (ANOVA) to determine if time-, rank-, treatment- effects had to be accounted for: $chl_{i,lf}$ started with similar values for all treatments and leaves at the time of leaf appearance and linearly increased till maximum chlorophyll content was reached. The increase rate was higher in HH than LL, and after FBV than before FBV for LH leaves expanding after FBV (Fig. S15). These functions describing chlorophyll temporal dynamics were applied to estimate chlorophyll dynamics in Exp. 1 from the leaf appearance dates in this treatment. $p_{i,lf}^{max}$ was set proportional to estimated $chl_{i,lf}$ (proportion coefficient estimated from Exp. 3 data).

Once estimated, the surfacic photosynthesis of each leaf, $P_{i,lf}$, was multiplied by leaf area, and each leaf photosynthesis summed, giving the total photosynthesis of the axis (Equation 5). C supply was obtained by multiplying photosynthesis by a conversion coefficient *c* that accounts for a 16h-photoperiod and a mean 20.6 °Cd per day according to Exp. 1 temperature measurements.

Demand estimation (Equations 6-8).

Firstly, $C_{i,org}^{struct}$ of each organ or compartment of each plant in Exp. 1 at each date was calculated as the difference between the measured total C mass (assuming 0.45 gC . gM^{-1}, M being dry mass) and the measured C mass allocated to soluble compounds (hexoses, sucrose, starch, amino acids, soluble proteins, and polyphenols). $C_{i,org}^{struct}$ for each leaf and for each internode was then divided by the measured leaf area or internode volume, respectively, to get the measured $CA_{i,lf}$ and $CV_{i,in}$ Secondly, a linear fitting procedure was applied on the measured $D_{i,in}$ $CA_{i,lf}$ $CV_{i,in}$ $C_{i,org}^{struct}$ (*org*= base, roots, flower) to obtain the temporal variation of these variables (Fig. S12-S14). This was preceded by a statistical analysis (ANOVA) to determine if time-, rank-, treatment- effects had to be accounted for. In all cases, similar initial values were taken for all organs and treatments when data were unsufficient to estimate these values. Finally, the demand was calculated for each

organ/compartment each 10°Cd, using equations 7 and 8 for individual leaves and internodes, and directly from the temporal variation of the other compartments.

Manipulation of source-sink balance (Exp. 4)

Sugar source for plants in HH and LL was artificially increased by exogenous sugar supply at FBV in zone Z3 where differences in bud outgrowth were strongly marked between light treatments. The terminal leaflet of the higher foliated leaf of zone Z3 was removed and the corresponding petiole was immersed in a aqueous solution (with 0.25% of Preservative Plant Mixture) of either 100mM sucrose or 50mM mannitol, an osmotic control, as made in Bertheloot et al. (2020).To avoid the diversion of sugar supplied in this way towards the actively growing apical organs, additional sucrose (100 mM) was vascularly supplied above Z3 (through the lowest internode of Z2), using the cotton wick-method described in Corot et al. (2017), for both petiole-fed sucrose and mannitol treatments (Fig. S1). This was done with the intention to feed the growing apical organs through a supply in Z2 and enable testing the effect of an increase in sugar locally in Z3.

Sugar source for plants in LH was artificially decreased by either masking the leaves or by applying a photosynthesis inhibitor. In the masking experiment, the upper surface of leaflets of all fully opened leaves were covered using either a black opaque (treated) or a transparent plastic film (control) from the fifth days after FBV. In the photosynthesis inhibition experiment, a solution containing DCMU (DCMU 50µM, 0.5% ethanol, Tween) or a similar solution without DCMU was applied once with a brush on half of each fully opened leaf from the sixth day after FBV. In addition, at FBV+7 days, photosynthesis was measured on leaf 4 (median leaflet) of treated and non-treated plants with DCMU to verify that photosynthesis was indeed decreased by DCMU application (data not shown).

For each treatment, the stage of development of each bud was recorded every two or three days.

Statistics and fitting procedures.

R software for Windows was used for statistical analyses, fitting procedures, and supply/demand calculation model.

The functions aov(), TukeyHSD(), fisher.test(), t.test() were used for analysis of variance (ANOVA), Tukey multiple comparison test, Fisher's exact test, Student's test, respectively. The functions geom_smooth(method='lm'), geom_smooth(), and geom_smooth(method = glm, method.args= list(family="binomial")) to estimate linear regressions, trends lines for continuous variables (*e.g.* time of bud outgrowth, chlorophyll) and for qualitative variable (bud outgrowth frequency), respectively.

The parameter estimations of specific functions (describing the temporal dynamics of chlorophyll, diameter, structural mass per unit area or volume, or PPFD attenuation with LAI, photosynthesis response to PPFD) was done by minimizing the root mean square errors between observations and estimations using the nlm() procedure.

Results

Continuous light limitation repressed axillary bud outgrowth, whereas transient light limitation overstimulated it and increased plant investment in bud outgrowth relative to primary axis growth.

In Experiment 1, single-axis rose plants derived from cuttings were grown under continuously high (*ca.* 420 µmol m^{-2} s^{-1}, HH), continuously low (*ca.* 90 µmol m^{-2} s^{-1}, LL), or transiently low light (Low-High: LH) with a shift to high light applied just before the onset of bud outgrowth at the floral bud visible stage

386 (FBV stage; Fig. 1). Each bud developmental status (dormant vs. outgrowing) and outgrowth timing
387 (referred to as "outgrowth date") were recorded along the primary axis. The axis was divided into an
388 apical zone (Z1; mainly including buds that do not enter dormancy), an intermediate zone (Z2), and a
389 basal zone (Z3; Fig. 2B).

390 Light treatments strongly affected bud outgrowth and branching (Fig. 2A-B). Under HH, bud outgrowth
391 (Fig. 2B) and branch development (Fig. 2A) were mainly restricted to Z1 and Z2 and followed a top-to-
392 bottom sequence in outgrowth dates (Fig. 2B). Under LL, this pattern was preserved but bud outgrowth
393 frequency was reduced in Z2 and Z3 (7% *vs.* 44% in HH on the entire axis). In contrast, LH induced
394 branching along the entire axis, with 98% of buds growing out in Z2 and Z3. Bud outgrowth was more
395 synchronous, resulting in a significant earlier mean bud outgrowth date all over the axis (146, 254, and
396 356 °Cd for LH, HH, and LL, respectively). These effects were confirmed in a second experiment
397 performed n a different growth chamber (Exp. 2; Fig. S2).

398 Because light is known to affect plant development (e.g., Chenu *et al.*, 2005; Gautier *et al.*, 1999), we
399 examined whether differences in bud outgrowth between light treatments were associated with
400 differences in primary axis growth. Dry mass of the different organs of the primary axis and roots was
401 quantified at several time points after FBV stage (floral bud visible at the axis top), and compared with
402 the bud outgrowth frequency cumulated along the primary axis (Fig. S2). Bud outgrowth frequency
403 was strongly related to dry mass accumulation for all light conditions, but LH displayed a stronger bud
404 outgrowth frequency increase relative to dry mass accumulation (Fig. 2C) indicating a higher relative
405 carbon allocation to axillary bud outgrowth under transient light limitation.

406 **Continuous light limitation decreased both starch and sucrose contents, while transient light**
407 **limitation promoted starch over-accumulation.**

408 To assess the relationship between light-dependent bud outgrowth patterns and sugar availability,
409 sucrose and starch were quantified in stems (internodes+nodes) and leaves of the median (Z2) and
410 basal (Z3) zones, which displayed clear differences in bud outgrowth accross treatments (Fig. 2B).
411 Sucrose and starch were used as indicators of sugar availability (Kool *et al.*, 1996), consistent with *in*
412 *vitro* rose stem segments experiments showing dose-dependent increases in starch and sucrose
413 concentrations with increasing external sucrose supply (Fig. S4; Barbier *et al.*, 2015b).

414 In experiment 1, samples were collected at three time points: (1) FBV (immediately after the light shift
415 in LH), (2) *ca.* 130 °Cd after FBV, corresponding to the onset of bud outgrowth in HH and LH, and (3)
416 after the end of bud outgrowth period for HH (*ca.* 400 °Cd) and LH (*ca.* 240 °Cd), and at its onset for LL
417 (*ca.* 290 °Cd) (Fig. 3A).

418 Under HH, sucrose and starch contents increased between FBV and the onset of bud outgrowth (*ca.*
419 130 °Cd), significantly for sucrose in Z2 and starch in Z3. During the subsequent bud outgrowth period,
420 they stabilized in stems and leaves, except for leaf starch that decrased. In LH, the increase in sucrose
421 and starch between BFV and *ca.* 130 °Cd was significant for both Z2 and Z3, with markedly higher starch
422 accumulation than in HH. Consequently, at the onset of bud outgrowth, LH plants had accumulated
423 more starch than HH plants, after which sugar levels stabilized or declined similarly to HH. In LL, sucrose
424 increased significantly only in leaves, while starch remained unchanged between FBV and *ca.* 130 °Cd
425 in leaves and stems; both sugars accumulated later in stems, between 130 °Cd and the onset of bud
426 outgrowth (*ca.* 290 °Cd). Overall, in all treatments, bud outgrowth started only after sucrose and starch
427 had accumulated in stems, with delayed accumulation in LL and enhanced starch accumulation in LH.

428 The second experiment (Exp. 2; Fig. 3B), focusing on the period before the onset of bud outgrowth
429 period in all treatments (*ca.* 8 days; Fig. S2), confirmed these patterns. Measurements were taken at

430 0, 4, and 7 days after FBV for HH and LH, and at 0 and 7 days for LL (using the same plants for LH and
431 LL at time 0, prior to the LH light shift). Starch accumulated more in LH than in HH, whereas neither
432 sucrose nor starch accumulated significantly in LL (except for sucrose in Z2, which remained lower than
433 in HH at day 7).

434 Together, these results reveal a strong correlation between bud outgrowth, and the dynamics of sugar
435 accumulation in stems, supporting a potential role for sugar availability in the light control of bud
436 outgrowth.

437 **Both continuous and transient light limitation reduced the photosynthetic capacity of mature leaves**
438 **after FBV.**

439 To determine whether differences in sugar availability between treatments were linked to
440 photosynthesis, a third experiment (Exp. 3) quantified the photosynthetic capacity of primary-axis
441 leaves under HH, LH, and LL (Fig. 4). Photosynthetic capacity reflects the ability of leaves to fix C and is
442 closely associated with nitrogen content, as a major component of the photosynthetic machinery
443 (Evans, 1989; Grindlay, 1997).

444 Net CO_2 assimilation was first measured, 3-4 days after FBV, on two fully-expanded basal leaves (ranks
445 1 and 4) under low (100 μmol m^{-2} s^{-1}) and high (600 μmol m^{-2} s^{-1}) photosynthetic photon flux density
446 (PPFD), and light response curves were fitted (Fig. 4A). Across treatments, older leaves (rank 1)
447 exhibited higher photosynthetic capacity than younger ones (rank 4), consistent with age-dependent
448 increases in nitrogen, RubisCo, and chlorophyll content during early leaf development (Osaki *et al.*,
449 1995). HH plants displayed higher photosynthetic capacity than LH and LL plants (Fig. 4A, C), indicating
450 a lasting acclimation to the lower light experienced during leaf expansion in LH (the four most basal
451 leaves had expanded under low light), as previously reported (Oguchi *et al.*, 2005; Sims and Pearcy,
452 1992).

453 To extend these observations to all leaves throughout their expansion, chlorophyll (Chl) index was used
454 as a proxy for leaf nitrogen content (Evans, 1989). As expected, in fully-expanded lower leaves (ranks
455 1 to 4), Chl index increased with leaf age (Fig. 4B) and was lower in LH and LL compared to HH (Fig. 4B
456 black and red, or Fig. 4D full lines). In upper expanding leaves, Chl index was lower than in mature
457 leaves for all treatments, increased over time and was: (i) slightly lower in LH than in HH, (ii) the lowest
458 in LL from day 7 onwards, *i.e.* before the onset of bud outgrowth (*ca.* 9 days). Thus, before bud
459 outgrowth, whole-axis photosynthetic capacity was reduced in both LH and LL compared to HH, mainly
460 due to lower photosynthetic capacity in mature basal leaves.

461 **Continuous light limitation reduced photosynthesis at the axis scale, but not transient light**
462 **limitation.**

463 At the whole-plant scale, photosynthesis depends on the photosynthetic capacity of individual leaves,
464 the PPFD they receive, and their area. Leaf area determines both the overall photosynthetic surface
465 and PPFD attenuation from the top to the bottom of the canopy (Varletgrancher *et al.*, 1989). We
466 therefore calculated primary-axis photosynthesis during the sugar accumulation period in Exp. 1 (FBV
467 to 300°Cd), using a model integrating these components (see Material and methods for calculation
468 details).

469 Leaf expansion was estimated using an existing model for the same rose cultivar (Demotes-Mainard et
470 al., 2013), fitted to our data. Lower mature leaves were the largest in LL, consistent with a shade
471 avoidance response (Grime, 1981), whereas upper expanding leaves were the smallest in LH (Fig. 5A).
472 HH plants also produced more leaves on average than LL and LH (Fig. S6).

473 Each leaf was assigned a photosynthetic capacity estimated on Chl indices and a PPFD environment
474 derived from the cumulated leaf area above it. As expected, PPFD was the lowest in LL due to low
475 incident light (Fig. 5B left). In contrast, despite receiving the same incident light as HH, LH plants
476 experienced higher PPFD at lower leaf levels owing to reduced shading from smaller upper leaf, a
477 pattern confirmed by direct measurements (Fig. S7; Exp. 3) and previous light simulations on Exp. 1
478 plants reconstructed in 3D (Demotes-Mainard *et al.*, 2025).

479 Using PPFD and photosynthetic capacity, surfacic photosynthesis was computed for each leaf (P_i in
480 equation (5); Fig. 5B right). PPFD differences primarily drove treatments effects, resulting in the lowest
481 surfacic photosynthesis in LL and the highest in LH. The reduced photosynthetic capacity in LH (Fig. 4)
482 therefore had little impact on surfacic photosynthesis compared with HH. Photosynthetic capacity
483 instead mainly affected surfacic photosynthesis during the period of leaf expansion, resulting in low
484 initial values for upper leaves (at °Cday), followed by increases as leaves expanded (at 150 and
485 300°Cday).

486 When multiplied by leaf area, surfacic photosynthesis estimates yielded absolute leaf photosynthesis
487 estimates (Fig. 5C). These were the lowest in LL, despite larger lower leaves, because of low PPFD.
488 Comparing LH with HH, basal leaves showed higher photosynthesis due to reduced self-shading, while
489 upper-leaf photosynthesis was lower because of smaller leaf size. Consequently, total primary-axis
490 photosynthesis was similar in LH and HH, but 3-6 times lower in LL (Fig. 5D). It increased over time with
491 leaf expansion for all treatments, although more slowly in LL due to PPFD limitation.

492 Thus, compared with HH, reduced sugar contents in LL can be explained by limited photosynthesis,
493 whereas sugar over-accumulation in LH cannot be attributed to increased photosynthetic activity.

494 **Transient light limitation before FBV reduced organ expansion after FBV.**

495 As reported for water stress (Muller *et al.*, 2011; Tardieu *et al.*, 1999), the sugar over-accumulation in
496 LH relative to HH could result from reduced organ expansion, lowering C demand while C supply from
497 photosynthesis remains similar, thus increasing supply-demand ratio.

498 In addition to the smaller estimated upper-leaf areas in LH compared with HH (Fig. 5A), measured
499 organ expansions between FBV and 130°Cd later (corresponding to the sugar accumulation period) in
500 Exp. 1 supported this hypothesis (Fig. 6). Upper leaves (relative rank > 0.55)– that appeared under low
501 light (Fig. S5)- expanded more in HH than in LL or LH (Fig. 6A), indicating that light conditions during
502 early developmental stages had a lasting effect on subsequent expansion. This aligns with previous
503 findings (Granier and Tardieu, 1999a) and with the reduced final area of upper leaves observed in LH
504 compared with HH in a separate experiment (Exp. 3; Fig. S8A). Internode development was also
505 affected by early light conditions: diameter was reduced in both LH and LL compared with HH (Fig. 6B;
506 Fig. S8B) while length showed a weaker but non-significant reduction in Exp. 1 (Fig. 6C; Fig. S8C).
507 Overall, shortly after FBV, both LH and LL plants exhibited reduced organ expansion compared with
508 HH, supporting the hypothesis that reduced expansion contributed to sugar over-accumulation in LH.

509 **Transient light limitation induces sugar accumulation due to reduced organ expansion, while**
510 **continuous light limitation reduces it through low photosynthesis.**

511 The combined estimations of photosynthesis and measurements of organ expansion (Fig. 5,6) support
512 the hypothesis that the reduced sugar accumulation observed in LL after FBV results from limited
513 photosynthesis and thus reduced C supply. Conversely, the sugar over-accumulation in LH appears to
514 result from reduced organ expansion, leading to lower C demand while C supply remains similar to HH.
515 This interpretation relies on two assumptions (i) in LL, the reduction in C demand by growing organs

516 does not compensate for the reduction in C supply; (ii) in LH, the reduction in C demand is sufficient to
517 increase the supply–demand ratio relative to HH. Testing these assumptions requires a quantitative
518 comparison of C supply and demand dynamics.

519 We estimated the temporal dynamics of C demand of all primary-axis organs every 10 °Cd from FBV to
520 300 °Cd (end of the sugar accumulation phase; Fig. 3) as the C required for structural growth. Structural
521 C growth was calculated as the product of organ expansion (leaf area increase or internode/peduncle
522 volume expansion) and structural C content per unit dimension (area, volume), with structural C
523 defined as total C minus soluble C compounds. Leaf expansion and internode/peduncle elongation
524 were estimated using a previously developed rose model (Demotes-Mainard *et al.*, 2013a) fitted to the
525 data from Exp. 1 (Fig. S10-S11). Internode and peduncle diameters, leaf structural mass per unit area,
526 and internode structural mass per unit volume were directly fitted on Exp. 1 measurements (Fig. S12-
527 14).

528 From these estimates, total leaf expansion, internode elongation, and to a lesser extent internode
529 thickening were found to be higher in HH than in LH or LL, consistent with Fig. 6, while internode
530 thickening was higher in LH than in LL (Fig. 7A). Leaf structural mass per unit area remained nearly
531 constant in LL and HH, but increased slightly in LH, suggesting a possible investment in structures
532 during expansion following the return to high light (Fig. S13). Internode structural mass increased
533 similarly across treatments and did not contribute to treatment differences in demand (Fig. S14).
534 Structural growth of roots, the flower, and secondary axes was included in total demand but did not
535 differ significantly between treatments (data not shown).

536 C demand was then calculated as the increment in total structural C between consecutive 10 °Cd steps
537 after FBV (Fig. 7B). Immediately after FBV, HH displayed the highest C demand, approximately 1.5 times
538 that of LH and LL. C subsequently decreased in HH and LL as organ expansion slowed (Fig. 7A). In LH, C
539 demand started at values similar to LL at FBV, reflecting reduced organ expansions under both
540 treatments, and remained relatively stable over time, reaching HH levels only around 200 °Cd. This
541 indicates that C demand was lower in LH than in HH during the period of sugar accumulation observed
542 in LH.

543 We next calculated the supply–demand balance by dividing photosynthetic C supply (Fig. 5D) by the
544 estimated C demand (Fig. 7C). From FBV till *ca.* 250 °Cd, both HH and LH showed increasing supply due
545 to expanding photosynthetic area (Fig. 5A, C), resulting in an increasing supply-demand balance
546 consistent with the accumulation of sucrose and starch (Fig. 3A). Compared to HH, LH displayed a
547 higher balance until *ca.* 200 °Cd primarily due to reduced demand, whereas LL consistently displayed
548 a lower balance as a result of reduced photosynthesis. These treatment-specific patterns matched the
549 observed sucrose and starch concentrations (Fig. 7C, symbols).

550 Together, these results quantitively validate our initial hypothesis: under continuous light limitation,
551 reduced sugar levels are explained by limited photosynthesis, whereas under transient light limitation,
552 enhanced sugar storage relative to HH results from reduced organ expansion and the associated
553 decline in C demand.

554 **C supply-demand balance contributes to establishing bud outgrowth differences between**
555 **treatments.**

556 We hypothesized that light-induced differences in the C supply-demand balance, and the resulting
557 differences in sugar availability, underlie the observed differences in bud outgrowth. To test this, in a
558 fourth experiment (Exp. 4), C balance was manipulated by either reducing supply in LH or increasing
559 supply in HH and LL.

In LH, C supply was reduced by either masking all fully expanded leaves of the primary axis after FBV or applying DCMU, a photosynthesis inhibitor. Leaf masking significantly reduced bud outgrowth frequencies in both the intermediate (Z2) and basal (Z3) zones (Fig. 8A). DCMU application also repressed bud outgrowth, although the effect was weaker and restricted to Z3 (Fig. 8B).

In HH and LL, C supply was increased by delivering exogenous sucrose through the petiole of the upper Z3 leaf after FBV. Mannitol was used as an osmotic control and, and an additional sucrose source was supplied above the application site to maintain sucrose delivery to upper sink organs. In both HH and LL, petiole-fed sucrose significantly stimulated bud outgrowth in Z3 compared with mannitol (Fig. 8C, D).

Together, these results demonstrate that treatment-dependent differences in bud outgrowth are causally linked to light-induced variations in the C supply–demand balance and the associated sugar availability.

Discussion

Bud outgrowth is strongly influenced by light intensity, yet the mechanisms underlying this effect remain unclear (Schneider *et al.*, 2019). In particular, the long-standing hypothesis -implemented in some ecophysiological models- that light-mediated control of bud outgrowth involves changes in sugar availability has never been directly tested. Although the promotive role of sugar availability in bud vicinity and related-signalling pathways is well-established (Barbier *et al.*, 2015a; Mason *et al.*, 2014), sugar availability involvement in light responses relies on correlative evidence and has been questioned in favour of cytokinins (CK) (Corot *et al.*, 2017; Roman *et al.*, 2016a). Furthermore, the mechanisms underlying the effects of transient low-light episodes remain unclear. Using a quantitative and dynamic analysis of source-sink relationships in single-axis rose plants, combined with source-sink perturbations, our study reveals that continuous and transient light limitation have contrasting effects on bud outgrowth -respectively inhibitory and stimulatory- through differential impacts on carbon (C) source and sink functions. The resulting changes in sugar availability within the plant axis contribute causally to bud outgrowth responses to light regimes.

Continuous and transient light limitation have contrasting effects on C availability, mainly through differential impacts on source and sink activities.

Reduced light intensity is classically associated with a decline in plant C status, reflected by lower sugar contents in organs or leaf mass per unit area (Bertin and Gary, 1998; Corot *et al.*, 2017; Furet *et al.*, 2014; Lafarge *et al.*, 2010; Proietti *et al.*, 2023; Savvides *et al.*, 2014; Tardieu *et al.*, 1999), consistent with the strong dependence of photosynthesis on irradiance (e.g., Hirose and Werger, 1987; Tardieu *et al.*, 1999). In agreement with this framework, continuous low light reduced sucrose and starch concentrations in the median and basal parts of the rose primary axis (Fig. 3). In contrast, the effects of transient light limitation are much less documented. Here, a short period of low light followed by a return to high light induced a strong increase in sucrose and starch immediately after the light shift, with starch levels reaching values up to six times higher than under continuous high light (Exp. 2, Fig. 3). Similar responses have been reported in rice leaves and sheaths following transient shading (Lafarge et al., 2010).

Because light intensity affects not only photosynthesis but also induces morphological and physiological adaptations (Chenu *et al.*, 2005; Grindlay, 1997; Jiang *et al.*, 2021), we conducted an integrated analysis to disentangle the respective contributions of C sources and sinks to plant C status.

604 C supply was estimated from individual leaf area and surfacic photosynthesis, driven by local light and
605 photosynthetic capacity, while C demand was approximated from structural growth. As expected,
606 continuous low light strongly reduced surfacic photosynthesis (Fig. 5, 7B, 7C). This was accompanied
607 by increased area of mature basal leaves, typical of shade-avoidance (Demotes-Mainard *et al.*, 2016)
608 (Fig. 5A), and reduced expansion of upper organs (Fig. 6). Although these morphological responses
609 slightly increased C supply and reduced demand, they were insufficient to compensate for the
610 limitation of surfacic photosynthesis, resulting in markedly reduced whole-axis photosynthesis
611 compared with continuous high light.

612 Our analysis also provides an explanation for the counterintuitive sugar accumulation observed after
613 transient light limitation. This accumulation resulted from a non-reversible inhibition of upper organ
614 expansion induced under low light, which persisted after the return to high light (Fig. 5A, 6) and
615 reduced C demand. This finding is consistent with observations showing that transient shading during
616 early leaf development irreversibly limits final leaf size by reducing the initial cell pool (Granier and
617 Tardieu, 1999a). Similar effects likely extend to monocots, where low light during the enclosed phase
618 of leaf development delays entry into rapid elongation and reduces final leaf size (Muller *et al.*, 2001).
619 In our study, this irreversible effect extended to internodes, whose length and diameter were reduced
620 by transient low light (Fig. 6B,C). Lower fully-expanded leaves were unaffected, likely because their
621 early development occurred before the light treatments, as they were preformed in the bud of the
622 original cutting (Girault *et al.*, 2010).
623 In contrast to C demand, C source capacity after transfer to high light was only slightly altered relative
624 to continuous high light (Fig. 5D). Reduced upper leaf area decreased self-shading and enhanced light
625 interception by lower leaves, while limiting photosynthesis of upper leaves (Fig. 5B,C). These
626 compensatory effects resulted in similar whole-axis photosynthesis between transient and continuous
627 high light conditions. Transient low light also induced non-reversible reductions in leaf photosynthetic
628 capacity (Fig. 4C,D), consistent with previous reports (Oguchi *et al.*, 2005; Sims and Pearcy, 1992) but
629 in our conditions, these physiological adaptations has a limited impact on whole-axis photosynthesis
630 (Fig. 5C).

631 **C availability as a determinant of light-mediated bud outgrowth regulation**

632 Evidence linking C availability to environmentally driven branching responses has mainly emerged from
633 cereal studies, based on correlations between tiller number and indicators of source–sink balance
634 under varying light and temperature conditions (Alam *et al.*, 2014; Alam *et al.*, 2017; Kim *et al.*, 2010).
635 In rose, biochemical approaches have provided more direct support for such a relationship (Corot *et*
636 *al.*, 2017; Furet *et al.*, 2014). Here, we show that transient low light strongly stimulated bud outgrowth,
637 whereas continuous low light inhibited it relative to continuous high light (Fig. 2) in parallel with
638 differences in sucrose and starch levels (Fig. 3). Our analysis further revealed that, under continuous
639 low light, bud outgrowth was delayed and occurred only after sufficient sugar accumulation in stems,
640 suggesting that a minimal C availability is required to trigger bud activation. This is consistent with *in*
641 *vitro* studies showing that a threshold sugar supply is required to overcome auxin-mediated inhibition
642 of bud outgrowth (Bertheloot *et al.*, 2020). In addition, under transient low light, the interval between
643 the outgrowth of successive buds along the axis was shortened (Fig. 2B), coinciding with strong sugar
644 accumulation. This acceleration explains the over-stimulation of bud outgrowth and branching at axis
645 scale (Fig. 2). A similar reduction in lag time before bud outgrowth has been reported for rose buds *in*
646 *vitro* under increased sugar availability (Barbier *et al.*, 2015a).

647 Recent studies have questioned the involvement of sugars in light-mediated bud regulation, as
648 exogenous sugar supply failed to restored branching in rose plants transferred to darkness or low light

649 (Corot *et al.*, 2017; Roman *et al.*, 2016a). Our results challenge this conclusion. Under transient low
650 light condition, reducing C source through leaf masking or photosynthetic inhibition inhibited bud
651 outgrowth, while under continuous low light, exogenous sugar supply promoted it (Fig. 8). Differences
652 with previous studies likely arise from experimental conditions and sugar application methods. In
653 Roman et al. (2016), plants were decapitated, defoliated, and placed in darkness, which may have
654 activated specific signalling pathways (Yoshida *et al.*, 2011). In Corot et al. (2017), very high sucrose
655 level was supplied through the petiole (300–800 mM) (Bertheloot *et al.*, 2020; Mason *et al.*, 2014)
656 which may have induced inhibitory effects, and vascular feeding (50-200 mM) may have preferentially
657 supplied apical sinks rather than buds. In contrast, our combined medium petiole and vascular feeding
658 strategy (100 mM sucrose) (Fig. S1) enabled moderate sugar supply to the bud while satisfying apical
659 demand, thereby promoting bud outgrowth.

660 Both Corot et al. (2017) and Roman et al. (2016) identified CK as mediators of light effects on bud
661 outgrowth, as CK levels decreased under low light and exogenous CK restored branching. Similar
662 conclusions were drawn for wheat tillering (Lorenzo *et al.*, 2015). I*n vitro* studies further show that
663 light or CK act synergistically with sugar availability to stimulate bud outgrowth : light or CK alone,
664 without sugar, cannot induce bud outgrowth, whereas sucrose enhanced CK effect for buds under
665 light, including in presence of auxin (Bertheloot *et al.*, 2020; Girault *et al.*, 2010; Jiang *et al.*, 2025;
666 Rabot *et al.*, 2012). This synergistic effect involves a stimulation of CK signalling, bud metabolism and
667 sink activity by sugar (Jiang *et al.*, 2025). Thus, two interacting pathways may coexist in light-mediated
668 bud regulation : a sugar- and a CK-dependent pathway. Such combined regulation has also been
669 reported for shoot apical meristems (Li *et al.*, 2017; Pfeiffer *et al.*, 2016).

670 **Key model requirements for simulating bud outgrowth regulation at the whole-plant scale**

671 Many whole-plant models simulate organ growth—and sometimes branch initiation—as a function of
672 plant C status, often through a C supply–demand balance (e.g. Drouet and Pages, 2007; Evers *et al.*,
673 2010; Guo *et al.*, 2006; Lescourret *et al.*, 2011; Luquet *et al.*, 2006; Pallas *et al.*, 2013). Our study
674 highlights requirements for models aiming to simulate branching responses to light intensity, including
675 transient low-light conditions.

676 Models must explicitly account for light history effects on organ development. Transient exposure to
677 low light during early developmental stage strongly limits subsequent organ expansion, even after
678 return to high light (Fig. 6,S8; Cookson *et al.*, 2005; Granier and Tardieu, 1999a), leading to reduced C
679 demand (Fig. 7A,B). When C supply is only weakly affected, as observed in our study, this creates a
680 decoupling between C supply (high) and demand (reduced), resulting in sugar over-accumulation and
681 enhanced bud outgrowth. In addition, C demand must be formalized as a function of organ expansion
682 rather than as an increase in mass, which also includes changes in dry mass par unit organ dimension.
683 The latter is linked to plant C status and so reflects the outcome of the source-sink balance rather than
684 the intrinsic demand of growing organs (Hilty *et al.*, 2021; Tardieu *et al.*, 1999). These requirements
685 may extend to the modelling of plant responses to water deficit, which similarly limits leaf expansion,
686 can increase plant C status, and was reported to stimulate branching upon stress release (Blum *et al.*,
687 1990; Demotes-Mainard *et al.*, 2013b; Granier and Tardieu, 1999b; Lecoeur *et al.*, 1995).

688 A major challenge, not addressed in the present study, is the formalization of bud outgrowth regulation
689 by C availability. Current models rely on empirical relationships between C status and branching,
690 implemented either at the whole-plant scale or at the level of individual buds with predefined windows
691 of bud sensitivity (Evers *et al.*, 2010; Hammer *et al.*, 2023; Luquet *et al.*, 2006). However, these
692 formalisms have rarely been evaluated against detailed experimental datasets and do not capture how
693 buds dynamically integrate C availability over time. Physiological evidence indicate that sugars act not

694 only as substrates but also as signaling molecules, activating within the bud pathways involving
695 trehalose-6-phosphate and hexokinase, sugar transporters, vacuolar invertase activity—a marker of
696 sink strength—, and metabolic pathways (Barbier *et al.*, 2021; Fichtner *et al.*, 2017; Fichtner *et al.*,
697 2020; Henry *et al.*, 2011; Wang *et al.*, 2021). Sugar signaling is also tightly interconnected with
698 hormonal regulation: high sugar availability represses strigolactone signaling and promotes CK
699 signaling, leading to repression of the dormancy-associated gene BRC1 (Bertheloot *et al.*, 2020; Patil
700 *et al.*, 2022)(Cao *et al.*, 2023; Jiang *et al.*, 2025)(Mason *et al.*, 2014; Wang *et al.*, 2019). Integrating this
701 mechanistic knowledge into a bud-scale model would represent a key step toward a physiologically
702 grounded representation of bud regulation by C availability. While Bertheloot et al (2020) proposed a
703 model describing the sugar–hormone interaction network controlling bud outgrowth, further
704 developments are now required to dynamically represent bud outgrowth for integration within
705 dynamic whole-plant models of branching plasticity.

706 **Conclusion**

707 Using a quantitative and dynamic modelling approach that captures source–sink responses to light
708 regimes and source–sink manipulations, we confirm that continuous low light intensity inhibits bud
709 outgrowth through reduced photosynthesis. We identify, for the first time, the mechanism underlying
710 the non-intuitive stimulatory effect of transient light limitation: a reduction in the growth—and thus C
711 use —of apical sink organs appearing under low light (Fig. 9). This mechanism may extend to other
712 environmental factors limiting sink growth, such as water deficit. Accurately simulating branching
713 plasticity therefore requires models that accurately represent both photosynthesis and the regulation
714 of C use by sink organs. This, in turn, calls for a better quantitative understanding of how bud
715 outgrowth regulators are dynamically integrated at the bud level. In addition to C, CK contribute to
716 light-mediated bud outgrowth and likely act as a complementary regulatory pathway. How C- and CK-
717 mediated controls interact remains an open question. Beyond light intensity, light quality—modulated
718 by canopy structure and controlled-environments—also affects branching and its interaction with light
719 quantity represents an important avenue for future research.

720

721 ## Supplementary data

722 Figure S1. Picture and scheme describing the method used for exogenous sugar supply.
723 Figure S2. Bud outgrowth along primary axes of rose plants grown under different light treatments in
724 Exp. 2.
725 Figure S3. Bud outgrowth and dry mass dynamics under the different light treatments.
726 Figure S4. Increasing sugar availability for bud-bearing stem segments *in vitro* promotes sucrose and
727 starch contents in the stem.
728 Figure S5. Leaf expansion periods for primary axes of plants grown in Exp. 3.
729 Figure S6. Final number of leaves in the different light treatments for Exp.1.
730 Figure S7. Measured PPFD at each leaf level after FBV for the different light treatments (Exp. 3).
731 Figure S8. Measured final organ dimensions for light treatments HH and LH (Exp. 3).
732 Figure S9. Variables used in equations 3-4 to estimate expansion kinetics of leaves and internodes for
733 primary axes of rose plants in Exp. 1 under HH, LH, LL.
734 Figure S10. Simulated and measured area expansions of individual leaves for each light treatment.
735 Figure S11. Simulated and measured elongations of individual internode and peduncle for each light
736 treatment.
737 Figure S12. Estimated and measured diameter increase of individual internodes and peduncle for each
738 light treatment.

Figure S13. Estimated and measured structural mass per unit area for individual leaves for each light treatment.

Figure S14. Estimated and measured structural mass per unit volume for individual internodes and peduncle for each light treatment.

Figure S15. Estimated and measured chlorophyll index for individual leaves in each light treatment for Exp. 3.

Acknowledgments

We thank Gérard Sintès for assistance with the growth chamber, Odile Douillet for help with plant growth, and Bénédicte Dubuc and the ImHorPhen team for rose production (UMR IRHS).

Author contribution

AS: Conceptualization, Visualization, Investigation, Methodology, Data curation, Formal analysis, Software, Writing-original draft. FB: Methodology, Writing-review & editing. SDM: Writing-original draft, Writing-review & editing. LL: Investigation, Methodology, Validation. MDPG: Investigation, Methodology, Visualization. CC: Investigation, Methodology. YG: Methodology, Supervision, Writing-review & editing. CG: Supervision, Conceptualization, Methodology, Writing-review & editing. SS: Funding acquisition, Supervision, Conceptualization, Writing-original draft, Writing-review & editing. JB: Funding acquisition, Project administration, Supervision, Conceptualization, Methodology, Formal analysis, Software, Data curation, Visualization, Writing-original draft, Writing-review & editing.

Conflict of interest

No conflict of interest declared.

Funding Statement

This work was supported by the National Research Institute for Agriculture, Food and Environment (INRAE), and the French region “Pays de la Loire”.

References

Alam MM, Hammer GL, van Oosterom EJ, Cruickshank AW, Hunt CH, Jordan DR. 2014. A physiological framework to explain genetic and environmental regulation of tillering in sorghum. New Phytologist **203**, 155-167.
Alam MM, van Oosterom EJ, Cruickshank AW, Jordan DR, Hammer GL. 2017. Predicting Tillering of Diverse Sorghum Germplasm across Environments. Crop Science **57**, 78-87.
Bantan-Polak T, Kassai M, Grant KB. 2001. A comparison of fluorescamine and naphthalene-2,3-dicarboxaldehyde fluorogenic reagents for microplate-based detection of amino acids. Analytical Biochemistry **297**, 128-136.
Barbier F, Lunn JE, Beveridge CA. 2015a. Ready, steady, go! A sugar hit starts the race to shoot branching. Current Opinion in Plant Biology **25**, 39-45.
Barbier F, Peron T, Lecerf M, Perez-Garcia MD, Barriere Q, Rolcik J, Boutet-Mercey S, Citerne S, Lemoine R, Porcheron B, Roman H, Leduc N, Le Gourrierec J, Bertheloot J, Sakr S. 2015b. Sucrose is an early modulator of the key hormonal mechanisms controlling bud outgrowth in Rosa hybrida. Journal of Experimental Botany **66**, 2569-2582.
Barbier FF, Cao D, Fichtner F, Weiste C, Perez-Garcia MD, Caradeuc M, Le Gourrierec J, Sakr S, Beveridge CA. 2021. HEXOKINASE1 signalling promotes shoot branching and interacts with cytokinin and strigolactone pathways. New Phytologist **231**, 1088-1104.
Barthelemy D, Caraglio Y. 2007. Plant architecture: A dynamic, multilevel and comprehensive approach to plant form, structure and ontogeny. Annals of Botany **99**, 375-407.
Baumont M, Parent B, Manceau L, Brown HE, Driever SM, Muller B, Martre P. 2019. Experimental and modeling evidence of carbon limitation of leaf appearance rate for spring and winter wheat. Journal of Experimental Botany **70**, 2449-2462.
Bertheloot J, Barbier F, Boudon F, Perez-Garcia MD, P?ron T, Citerne S, Dun E, Beveridge C, Godin C, Sakr S. 2020. Sugar availability suppresses the auxin-induced strigolactone pathway to promote bud outgrowth. New Phytologist **225**, 866-879.
Bertheloot J, Cournede PH, Andrieu B. 2011. NEMA, a functional-structural model of nitrogen economy within wheat culms after flowering. I. Model description. Annals of Botany **108**, 1085-1096.
Bertin N, Gary C. 1998. Short and long term fluctuations of the leaf mass per area of tomato plants - Implications for growth models. Annals of Botany **82**, 71-81.
Blum A, Ramaiah S, Kanemasu ET, Paulsen GM. 1990. WHEAT RECOVERY FROM DROUGHT STRESS AT THE TILLERING STAGE OF DEVELOPMENT. Field Crops Research **24**, 67-85.
Borrell AK, Mullet JE, George-Jaeggli B, van Oosterom EJ, Hammer GL, Klein PE, Jordan DR. 2014. Drought adaptation of stay-green sorghum is associated with canopy development, leaf anatomy, root growth, and water uptake. Journal of Experimental Botany **65**, 6251-6263.
Bos HJ, Neuteboom JH. 1998. Morphological analysis of leaf and tiller number dynamics of wheat (Triticum aestivum L.): Responses to temperature and light intensity. Annals of Botany **81**, 131-139.
Boumaza R, Huché-Thélier L, Demotes-Mainard S, Le Coz E, Leduc N, Pelleschi-Travier S, Qannari E, Sakr S, Santagostini P, Symoneaux R, Guérin V. 2010. Sensory profiles and preference analysis in ornamental horticulture: The case of the rosebush. . Food Quality and Preference.
Bradford MM. 1976. RAPID AND SENSITIVE METHOD FOR QUANTITATION OF MICROGRAM QUANTITIES OF PROTEIN UTILIZING PRINCIPLE OF PROTEIN-DYE BINDING. Analytical Biochemistry **72**, 248-254.
Cao D, Chabikwa T, Barbier F, Dun EA, Fichtner F, Dong LL, Kerr SC, Beveridge CA. 2023. Auxin-independent effects of apical dominance induce changes in phytohormones correlated with bud outgrowth. Plant Physiology.
Cerovic ZG, Masdoumier G, Ben Ghozlen N, Latouche G. 2012. A new optical leaf-clip meter for simultaneous non-destructive assessment of leaf chlorophyll and epidermal flavonoids. Physiologia Plantarum **146**, 251-260.

Chenu K, Franck N, Dauzat J, Barczi JF, Rey H, Lecoeur J. 2005. Integrated responses of rosette organogenesis, morphogenesis and architecture to reduced incident light in Arabidopsis thaliana results in higher efficiency of light interception. Functional Plant Biology **32**, 1123-1134.
Cline MG. 1991. APICAL DOMINANCE. Botanical Review **57**, 318-358.
Colombié S, Prigent S, Cassan C, Hilbert-Masson G, Renaud C, Dell'Aversana E, Carillo P, Moing A, Beaumont C, Beauvoit B, McCubbin T, Nielsen LK, Gibon Y. 2023. Comparative constraint-based modelling of fruit development across species highlights nitrogen metabolism in the growth-defence trade-off. Plant Journal **116**, 786-803.
Cookson SJ, Van Lijsebettens M, Granier C. 2005. Correlation between leaf growth variables suggest intrinsic and early controls of leaf size in Arabidopsis thaliana. Plant Cell and Environment **28**, 1355-1366.
Corot A, Roman H, Douillet O, Autret H, Perez-Garcia MD, Citerne S, Bertheloot J, Sakr S, Leduc N, Demotes-Mainard S. 2017. Cytokinins and Abscisic Acid Act Antagonistically in the Regulation of the Bud Outgrowth Pattern by Light Intensity. Frontiers in Plant Science **8**.
Crespel L, Le Bras C, Amoroso T, Ulloa MGU, Morel P, Sakr S. 2020. Genotype x Light Quality Interaction on Rose Architecture. Agronomy-Basel **10**.
Cross JM, von Korff M, Altmann T, Bartzetko L, Sulpice R, Gibon Y, Palacios N, Stitt M. 2006. Variation of enzyme activities and metabolite levels in 24 arabidopsis accessions growing in carbon-limited conditions. Plant Physiology **142**, 1574-1588.
Demotes-Mainard S, Autret H, Pradal C, Le Gall J, Guérin V, Leduc N, Combes D, Renaud C, Chelle M, Bertheloot J. 2025. Simulating light quantity and quality over plant organs using a ray-tracing method to investigate plant responses in growth chambers. Biosystems Engineering **258**.
Demotes-Mainard S, Bertheloot J, Boumaza R, Huche-Thelier L, Gueritaine G, Guerin V, Andrieu B. 2013a. Rose bush leaf and internode expansion dynamics: analysis and development of a model capturing interplant variability. Frontiers in Plant Science **4**.
Demotes-Mainard S, Huché-Thélier L, Morel P, Boumaza R, Guérin V, Sakr S. 2013b. Temporary water restriction or light intensity limitation promotes branching in rosebush. Scientia Horticulturae **150**, 432-440.
Demotes-Mainard S, Peron T, Corot A, Bertheloot J, Le Gourrierec J, Pelleschi-Travier S, Crespel L, Morel P, Huche-Thelier L, Boumaza R, Vian A, Guerin V, Leduc N, Sakr S. 2016. Plant responses to red and far-red lights, applications in horticulture. Environmental and Experimental Botany **121**, 4-21.
Domagalska MA, Leyser O. 2011. Signal integration in the control of shoot branching. Nature Reviews Molecular Cell Biology **12**, 211-221.
Dong M. 1995. MORPHOLOGICAL RESPONSES TO LOCAL LIGHT CONDITIONS IN CLONAL HERBS FROM CONTRASTING HABITATS, AND THEIR MODIFICATION DUE TO PHYSIOLOGICAL INTEGRATION. Oecologia **101**, 282-288.
Drouet JL, Pages L. 2007. GRAAL-CN: A model of GRowth, Architecture and ALlocation of Carbon and Nitrogen dynamics within whole plants formalised at the organ level. Ecological Modelling **206**, 231-249.
Evans JR. 1989. PHOTOSYNTHESIS AND NITROGEN RELATIONSHIPS IN LEAVES OF C-3 PLANTS. Oecologia **78**, 9-19.
Evers JB, Vos J, Yin X, Romero P, van der Putten PEL, Struik PC. 2010. Simulation of wheat growth and development based on organ-level photosynthesis and assimilate allocation. Journal of Experimental Botany **61**, 2203-2216.
Fichtner F, Barbier F, Feil R, Watanabe M, Annunziata MG, Chabikwa TG, Höfgen R, Stitt M, Beveridge CA, Lunn JE. 2017. Trehalose 6-phosphate is involved in triggering axillary bud outgrowth in garden pea (Pisum sativum L.). The Plant Journal **92**, 611-623.
Fichtner F, Olas JJ, Feil R, Watanabe M, Krause U, Hoefgen R, Stitt M, Lunn JE. 2020. Functional Features of TREHALOSE-6-PHOSPHATE SYNTHASE1, an Essential Enzyme in Arabidopsis(OPEN). Plant Cell **32**, 1949-1972.
Furet PM, Lothier J, Demotes-Mainard S, Travier S, Henry C, Guerin V, Vian A. 2014. Light and nitrogen nutrition regulate apical control in Rosa hybrida L. Journal of Plant Physiology **171**, 7-13.

Garcia-Martinez JL, Gil J. 2001. Light regulation of gibberellin biosynthesis and mode of action. Journal of Plant Growth Regulation **20**, 354-368.
Gautier H, Varlet-Grancher C, Hazard L. 1999. Tillering responses to the light environment and to defoliation in populations of perennial ryegrass (Lolium perenne L.) selected for contrasting leaf length. Annals of Botany **83**, 423-429.
Girault T, Abidi F, Sigogne M, Pelleschi-Travier S, Boumaza R, Sakr S, Leduc N. 2010. Sugars are under light control during bud burst in Rosa sp. Plant, Cell & Environment **33**, 1339-1350.
Granier C, Tardieu F. 1999a. Leaf expansion and cell division are affected by reducing absorbed light before but not after the decline in cell division rate in the sunflower leaf. Plant Cell and Environment **22**, 1365-1376.
Granier C, Tardieu F. 1999b. Water deficit and spatial pattern of leaf development. Variability in responses can be simulated using a simple model of leaf development. Plant Physiology **119**, 609-619.
Grime J. 1981. *Plant strategies in shade.* London: Academic press.
Grindlay DJC. 1997. Towards an explanation of crop nitrogen demand based on the optimization of leaf nitrogen per unit leaf area. Journal of Agricultural Science **128**, 377-396.
Guo Y, Ma YT, Zhan ZG, Li BG, Dingkuhn M, Luquet D, De Reffye P. 2006. Parameter optimization and field validation of the functional-structural model GREENLAB for maize. Annals of Botany **97**, 217-230.
Hammer GL, McLean G, Kholová J, van Oosterom E. 2023. Modelling the dynamics and phenotypic consequences of tiller outgrowth and cessation in sorghum. In Silico Plants **5**.
Hendriks JHM, Kolbe A, Gibon Y, Stitt M, Geigenberger P. 2003. ADP-glucose pyrophosphorylase is activated by posttranslational redox-modification in response to light and to sugars in leaves of Arabidopsis and other plant species. Plant Physiology **133**, 838-849.
Henry C, Rabot A, Laloi M, Mortreau E, Sigogne M, Leduc N, Lemoine R, Sakr S, Vian A, Pelleschi-Travier S. 2011. Regulation of RhSUC2, a sucrose transporter, is correlated with the light control of bud burst in Rosa sp. Plant Cell and Environment **34**, 1776-1789.
Hilty J, Muller B, Pantin F, Leuzinger S. 2021. Plant growth: the What, the How, and the Why. New Phytologist **232**, 25-41.
Hirose T, Werger MJA. 1987. NITROGEN USE EFFICIENCY IN INSTANTANEOUS AND DAILY PHOTOSYNTHESIS OF LEAVES IN THE CANOPY OF A SOLIDAGO-ALTISSIMA STAND. Physiologia Plantarum **70**, 215-222.
Hitz T, Hartung J, Graeff-Honninger S, Munz S. 2019. Morphological Response of Soybean (Glycine max (L.) Merr.) Cultivars to Light Intensity and Red to Far-Red Ratio. Agronomy-Basel **9**.
Jiang YP, Ding XT, Wang JY, Zou J, Nie WF. 2021. Decreased low-light regulates plant morphogenesis through the manipulation of hormone biosynthesis in Solanum lycopersicum. Environmental and Experimental Botany **185**.
Jiang ZR, Wang M, Gouaille L, Barbier F, Nicolas M, Wang YH, Pérez-Garcia MD, Ogé L, Ledroit L, Cukier C, Lalande J, Hamama L, Crespel L, Ding YF, Lothier J, Le Gourrierec J, Bertheloot J, Li GH, Sakr S. 2025. Cytokinin-induced bud outgrowth depends on sugar metabolism and signalling. Journal of Experimental Botany **76**, 5351-5366.
Kebrom TH, Chandler PM, Swain SM, King RW, Richards RA, Spielmeyer W. 2012. Inhibition of Tiller Bud Outgrowth in the tin Mutant of Wheat Is Associated with Precocious Internode Development. Plant Physiology **160**, 308-318.
Kebrom TH, Mullet JE. 2015. Photosynthetic leaf area modulates tiller bud outgrowth in sorghum. Plant Cell and Environment **38**, 1471-1478.
Kim HK, van Oosterom E, Dingkuhn M, Luquet D, Hammer G. 2010. Regulation of tillering in sorghum: environmental effects. Annals of Botany **106**, 57-67.
Kool MTN, Westerman AD, RouHaest CHM. 1996. Importance and use of carbohydrate reserves in above-ground stem parts of rose cv Motrea. Journal of Horticultural Science & Biotechnology **71**, 893-900.

Lafarge T, Seassau C, Martin M, Bueno C, Clement-Vidal A, Schreck E, Luquet D. 2010. Regulation and recovery of sink strength in rice plants grown under changes in light intensity. Functional Plant Biology **37**, 413-428.
Lang GA, Early JD, Martin GC, Darnell RL. 1987. ENDODORMANCY, PARADORMANCY, AND ECODORMANCY - PHYSIOLOGICAL TERMINOLOGY AND CLASSIFICATION FOR DORMANCY RESEARCH. Hortscience **22**, 371-377.
Lecoeur J, Wery J, Turc O, Tardieu F. 1995. EXPANSION OF PEA LEAVES SUBJECTED TO SHORT WATER-DEFICIT - CELL NUMBER AND CELL-SIZE ARE SENSITIVE TO STRESS AT DIFFERENT PERIODS OF LEAF DEVELOPMENT. Journal of Experimental Botany **46**, 1093-1101.
Leduc N, Roman H, Barbier F, Péron T, Huché-Thélier L, Lothier J, Demotes-Mainard S, Sakr S. 2014. Light signaling in bud outgrowth and branching in plants. Plants **3**, 223-250.
Lescourret F, Moitrier N, Valsesia P, Genard M. 2011. QualiTree, a virtual fruit tree to study the management of fruit quality. I. Model development. Trees-Structure and Function **25**, 519-530.
Li XJ, Cai WG, Liu YL, Li H, Fu LW, Liu ZY, Xu L, Liu HT, Xu TD, Xiong Y. 2017. Differential TOR activation and cell proliferation in Arabidopsis root and shoot apexes. Proceedings of the National Academy of Sciences of the United States of America **114**, 2765-2770.
Lorenzo M, Assuero SG, Tognetti JA. 2015. Low temperature differentially affects tillering in spring and winter wheat in association with changes in plant carbon status. Annals of Applied Biology **166**, 236-248.
Luquet D, Dingkuhn M, Kim H, Tambour L, Clement-Vidal A. 2006. EcoMeristem, a model of morphogenesis and competition among sinks in rice. 1. Concept, validation and sensitivity analysis. Functional Plant Biology **33**, 309-323.
Mason MG, Ross JJ, Babst BA, Wienclaw BN, Beveridge CA. 2014. Sugar demand, not auxin, is the initial regulator of apical dominance. Proceedings of the National Academy of Sciences of the United States of America **111**, 6092-6097.
Mathieu A, Cournede PH, Letort V, Barthelemy D, de Reffye P. 2009. A dynamic model of plant growth with interactions between development and functional mechanisms to study plant structural plasticity related to trophic competition. Annals of Botany **103**, 1173-1186.
Milthorpe FL, Newton P. 1963. STUDIES ON EXPANSION OF LEAF SURFACE .3. INFLUENCE OF RADIATION ON CELL DIVISION AND LEAF EXPANSION. Journal of Experimental Botany **14**, 483-&.
Mitchell KJ. 1953a. Influence of Light and Temperature on the Growth of Ryegrass (Lolium spp.). I. Pattern of vegetative development. Physiologia Plantarum **6**, 21-46.
Mitchell KJ. 1953b. Influence of Light and Temperature on the Growth of Ryegrass (Lolium spp.). II. The control of Lateral Bud Development. Physiologia Plantarum **6**, 425-443.
Muller B, Pantin F, Genard M, Turc O, Freixes S, Piques M, Gibon Y. 2011. Water deficits uncouple growth from photosynthesis, increase C content, and modify the relationships between C and growth in sink organs. Journal of Experimental Botany **62**, 1715-1729.
Muller B, Reymond M, Tardieu F. 2001. The elongation rate at the base of a maize leaf shows an invariant pattern during both the steady-state elongation and the establishment of the elongation zone. Journal of Experimental Botany **52**, 1259-1268.
Noia RD, Jr., Deswarte JC, Cohan JP, Martre P, van der Velde M, Lecerf R, Webber H, Ewert F, Ruane AC, Slafer GA, Asseng S. 2023. The extreme 2016 wheat yield failure in France. Global Change Biology **29**, 3130-3146.
Oguchi R, Hikosaka K, Hirose T. 2005. Leaf anatomy as a constraint for photosynthetic acclimation: differential responses in leaf anatomy to increasing growth irradiance among three deciduous trees. Plant Cell and Environment **28**, 916-927.
Osaki M, Iyoda M, Tadano T. 1995. ONTOGENIC CHANGES IN THE CONTENTS OF RIBULOSE-1,5-BISPHOSPHATE CARBOXYLASE OXYGENASE, PHOSPHOENOLPYRUVATE CARBOXYLASE AND CHLOROPHYLL IN INDIVIDUAL LEAVES OF MAIZE. Soil Science and Plant Nutrition **41**, 285-293.
Pallas B, Clement-Vidal A, Rebolledo MC, Soulie JC, Luquet D. 2013. Using plant growth modeling to analyze C source-sink relations under drought: inter- and intraspecific comparison. Frontiers in Plant Science **4**.

Patil SB, Barbier FF, Zhao JF, Zafar SA, Uzair M, Sun YL, Fang JJ, Perez-Garcia MD, Bertheloot J, Sakr S, Fichtner F, Chabikwa TG, Yuan SJ, Beveridge CA, Li XY. 2022. Sucrose promotes D53 accumulation and tillering in rice. New Phytologist **234**, 122-136.
Pfeiffer A, Janocha D, Dong YH, Medzihradszky A, Schöne S, Daum G, Suzaki T, Forner J, Longenecker T, Rempel E, Schmid M, Wirtz M, Hell R, Lohmann JU. 2016. Integration of light and metabolic signals for stem cell activation at the shoot apical meristem. Elife **5**.
Proietti S, Paradiso R, Moscatello S, Saccardo F, Battistelli A. 2023. Light Intensity Affects the Assimilation Rate and Carbohydrates Partitioning in Spinach Grown in a Controlled Environment. Plants-Basel **12**.
Rabot A, Henry C, Ben Baaziz K, Mortreau E, Azri W, Lothier J, Hamama L, Boummaza R, Leduc N, Pelleschi-Travier S, Le Gourrierec J, Sakr S. 2012. Insight into the Role of Sugars in Bud Burst Under Light in the Rose. Plant and Cell Physiology **53**, 1068-1082.
Roman H, Girault T, Barbier F, Peron T, Brouard N, Pencik A, Novak O, Vian A, Sakr S, Lothier J, Le Gourrierec J, Leduc N. 2016a. Cytokinins Are Initial Targets of Light in the Control of Bud Outgrowth(1 OPEN). Plant Physiology **172**, 489-509.
Roman H, Girault T, Barbier F, Péron T, Brouard N, Pencik A, Novak O, Vian A, Sakr S, Lothier J, Le Gourrierec J, Leduc N. 2016b. Cytokinins are initial targets of light in the control of bud outgrowth. Plant Physiology **172**, 489-509.
Savvides A, Ntagkas N, van Ieperen W, Dieleman JA, Marcelis LFM. 2014. Impact of light on leaf initiation: a matter of photosynthate availability in the apical bud? Functional Plant Biology **41**, 547-556.
Schneider A, Godin C, Boudon F, Demotes-Mainard S, Sakr S, Bertheloot J. 2019. Light Regulation of Axillary Bud Outgrowth Along Plant Axes: An Overview of the Roles of Sugars and Hormones. Frontiers in Plant Science **10**.
SharathKumar M, Heuvelink E, Marcelis LFM. 2020. Vertical Farming: Moving from Genetic to Environmental Modification. Trends in Plant Science **25**, 724-727.
Sims DA, Pearcy RW. 1992. RESPONSE OF LEAF ANATOMY AND PHOTOSYNTHETIC CAPACITY IN ALOCASIA-MACRORRHIZA (ARACEAE) TO A TRANSFER FROM LOW TO HIGH LIGHT. American Journal of Botany **79**, 449-455.
Slafer GA, Savin R, Sadras VO. 2014. Coarse and fine regulation of wheat yield components in response to genotype and environment. Field Crops Research **157**, 71-83.
Stitt M, Lilley RM, Gerhardt R, Heldt HW. 1989. METABOLITE LEVELS IN SPECIFIC CELLS AND SUBCELLULAR COMPARTMENTS OF PLANT-LEAVES. Methods in Enzymology **174**, 518-552.
Su HW, Abernathy SD, White RH, Finlayson SA. 2011. Photosynthetic photon flux density and phytochrome B interact to regulate branching in Arabidopsis. Plant Cell and Environment **34**, 1986-1998.
Tabourel-Tayot F, Gastal F. 1998. MecaNiCAL, a supply-demand model of carbon and nitrogen partitioning applied to defoliated grass 1. Model description and analysis. European Journal of Agronomy **9**, 223-241.
Tardieu F, Granier C, Muller B. 1999. Modelling leaf expansion in a fluctuating environment: are changes in specific leaf area a consequence of changes in expansion rate? New Phytologist **143**, 33-44.
Thimann KV, Skoog F. 1933. Studies on the growth hormone of plants. III. The inhibitory action of the growth substance on bud development. Proc. Natl. Acad. Sci.USA **19**, 714-716.
Thornley JHM. 1998. Dynamic model of leaf photosynthesis with acclimation to light and nitrogen. Annals of Botany **81**, 421-430.
Tschoep H, Gibon Y, Carillo P, Armengaud P, Szecowka M, Nunes-Nesi A, Fernie AR, Koehl K, Stitt M. 2009. Adjustment of growth and central metabolism to a mild but sustained nitrogen-limitation in Arabidopsis. Plant Cell and Environment **32**, 300-318.
Varletgrancher C, Gosse G, Chartier M, Sinoquet H, Bonhomme R, Allirand JM. 1989. SOLAR-RADIATION ABSORBED OR INTERCEPTED BY A CROP. Agronomie **9**, 419-439.

Wang M, Le Moigne MA, Bertheloot J, Crespel L, Perez-Garcia MD, Oge L, Demotes-Mainard S, Hamama L, Daviere JM, Sakr S. 2019. BRANCHED1: A Key Hub of Shoot Branching. Frontiers in Plant Science **10**.
Wang M, Ogé L, Garcia MDP, Launay-Avon A, Clément G, Le Gourrierec J, Hamama L, Sakr S. 2022. Antagonistic Effect of Sucrose Availability and Auxin on Rosa Axillary Bud Metabolism and Signaling, Based on the Transcriptomics and Metabolomics Analysis. Frontiers in Plant Science **13**.
Wang M, Perez-Garcia MD, Daviere JM, Barbier F, Oge L, Gentilhomme J, Voisine L, Peron T, Launay-Avon A, Clement G, Baumberger N, Balzergue S, Macherel D, Grappin P, Bertheloot J, Achard P, Hamama L, Sakr S. 2021. Outgrowth of the axillary bud in rose is controlled by sugar metabolism and signalling. Journal of Experimental Botany **72**, 3044-3060.
Warren-Wilson J. 1972. Control of crop processes. *Crop processes in Controlled Environments*. London: Academic Press, 7-30.
Yoshida S, Mandel T, Kuhlemeier C. 2011. Stem cell activation by light guides plant organogenesis. Genes & Development **25**, 1439-1450.

Figure legends

Figure 1. Light treatments applied to rose plants during their development. From plant emergence from a single-node cutting, plants were rapidly transferred to a growth chamber where they were submitted to different regimes of light intensity: (i) LL (Low-Low, grey strip): a constant low light intensity; (ii) HH (High-High, orange strip): a constant high light intensity; (iii) LH (Low-High): a temporary light limitation until the floral bud becomes visible at the top of the primary axis (FBV stage), i.e. before axillary buds started to grow out. *FBV:* floral bud visible; *PCV*: petal color visible; *OF*: opened flower: *FF*: faded flower.

Figure 2. Axillary bud outgrowth was repressed by continuous light limitation but stimulated by transient light limitation compared to continuous high light. (***A***) Pictures of a rose plant at opened or faded flower stage (*OF*). White arrows represent lateral branches. (***B***) Outgrowth frequency and date (expressed as degree days after FBV) for buds at different ranks along the primary axis of rose plants grown under HH (red), LH (green), and LL (blue), in Exp. 1. Rank is expressed relative to the total number of leaves and assigned to a zone (Z1, Z2, Z3; see material and methods). For date, only ranks with a rate > 0.2 are represented. Lines represent logistic and loess smooth lines, respectively, ± 95% confidence intervals (*n*=15 plants for LH and 20 plants for HH, LL). (***C***) Relationship between (i) primary axis and root dry mass and (ii) bud outgrowth frequency for plants grown under HH, LH, and LL. Data are identical to Fig. S3 data. Symbols represent means for each variable, errors bars represent SEM, and lines the estimated linear regression between dry mass and bud outgrowth frequency for each light condition.

Figure 3. Sucrose and starch levels were reduced after FBV by continuous light limitation but stimulated by transient light limitation. Temporal dynamics of sucrose and starch for zones Z2 and Z3 of rose plants grown under HH (red), LH (green), or LL (blue) in Exp. 1 (***A***) and Exp. 2 (***B***). In (*A*), sugars were quantified in the leaves or internodes+nodes of each zone all over primary axis growth, including bud outgrowth period; horizontal arrows indicate bud outgrowth period, with the start of the arrow being the date at which bud outgrowth starts in Z2. Data are means ± SEM (*n*=4-5 plants). Time is expressed in degree days to account for the slight difference in temperature between the two growth chambers where low and high PPFD were applied, respectively. In (*B*), sugars were quantified in the leaves or nodes of each zone, specifically before the beginning of bud outgrowth. Data are means ± SEM of 4 repetitions of at least four pooled plants each. Time is expressed in days. For (*A*,*B*), different letters indicate significant differences between treatments and sampling dates (ANOVA followed by a Tukey test, $p < 0.05$). In (*B*), no measurement was made for LL plants at time=0 considering an identical value to LH plants (shifted to high light just after time 0; blue letter written but identical to the green letter).

Figure 4. Leaf photosynthesis capacity was reduced after FBV for continuous and temporary light limitation. (***A***) Measured (symbols) and fitted (lines) CO_2 net assimilation of mature leaves 1 (black) and 4 (grey), counting from base, of rose primary axes grown under HH, LH, or LL in Exp. 3. Measurements were made 3 or 4 days after FBV at a PPFD at leaf level of 100 or 600 μmol m^{-2} s^{-1}, and are means ± SEM of 5 plants. Asterisks indicate significant differences between leaf ranks at each PPFD level (Student's test, p<0.05). Estimations were made by fitting a rectangular hyperbola (Equation 5). (***B***) Measured chlorophyll index as a function of time from FBV for each leaf rank (each line). Data represent loess regressions ± 95% confidence intervals (*n*=15-17 leaves). The brown vertical arrow represents the date at which net assimilation was measured in (*A*). (***C***) Focus on the measured net assimilation at 600 μmol m^{-2} s^{-1} of (A). Different letters indicate a significant difference between ranks and light treatments (pairwise comparison using Tukey test; *P*<0.05). (***D***) Overall chlorophyll index

dynamics for the lower fully-expanded leaves (ranks <=4) and the upper expanding ones (ranks >4; *D*; Fig. S5). Data represent loess regressions ± 95% confidence intervals (*n*=45-68 leaves). The vertical dashed grey line represents the date at which bud outgrowth started.

Figure 5. Estimated photosynthesis at primary axis scale was reduced by continuous but not temporary light limitation. Estimated temporal dynamics - between 0 and 300 °Cd - of the photosynthesis determinants and of photosynthesis of primary axes of rose plants grown under HH, LH, or LL in Exp. 1. (***A***) Leaf areas, (***B***) local PPFD and surfacic photosynthesis, (***C***) absolute photosynthesis of individual leaves along the primary axis at 0, 150, and 300 °Cd, and (***D***) photosynthesis of the primary axis through time. Methods for estimations are detailed in material and methods. The estimated primary axes had 9, 8, 8 leaves for HH, LH, LL, respectively, according to the median total number of leaves in each light treatment.

Figure 6. Low light, either continuously or transiently applied, reduced the increase in dimensions of primary axis organs after FBV. Increase - between FBV stage and FBV + *ca.* 130 °Cd - in the leaf area (***A***), the internode diameter (***B***), and the internode length (***C***) according to organ relative rank, for rose primary axes grown under HH, LH, or LL in Exp. 1. The period between FBV stage and FBV + *ca.* 130 °Cd was characterized by sugar accumulation in HH, LH. The horizontal dashed line separates the upper expanding organs to the bottom fully-expanded ones. For each treatment, organs were pooled in 8 groups according to their relative position (see M&M) from plant base. For each group, data are the mean ± SEM of the differences between values at FBV + *ca.* 130 °Cd and the mean value at FBV (*n*= 4-5 plants). Different letters indicate significant differences between treatments (ANOVA followed by a Tukey test, $p < 0.05$).

Figure 7. Continuous and temporary light limitation reduced C demand after FBV, and respectively repressed and stimulated C supply-demand balance just after FBV. (***A***) Estimated temporal dynamics - from FBV till 300 °Cd - of components for structural mass estimation of primary axes of Exp. 1 rose plants under HH, LH, or LL: leaf areas, internode/peduncle lengths and diameters. Data on individual organs were cumulated and expressed relatively to values at 0°Cd for lisibility. Estimations for individual organs are presented Fig. S10 to S14. (***B***) Derived estimated temporal dynamics of C demand. (***C***) Derived supply-demand ratio (lines) and measured internode sucrose+starch contents (Z2+Z3; symbols). Sugar contents were means ± SEM (*n*=4-5 plants; data similar to Fig. 3). Methods for estimations are detailed in material and methods. The simulated primary axes had 9, 8, 8 leaves for HH, LH, LL, respectively, according to the median total number of leaves in each light treatment.

Figure 8. Changes of C supply induced disruptions in bud outgrowth response to light. (***A***, ***B***) Bud outgrowth rate in the three zones along rose primary axes grown under LH with photosynthesis either not decreased (control) or decreased: (*A*) by covering fully opened leaves with either a black plastic (masked) or a transparent film (control) (*B*) or by applying 100 µM DCMU. (***C***,***D***) Bud outgrowth rate in the three zones along rose primary axes grown under HH (*C*) or LL (*D*) and supplied with either 50 mM mannitol (control) or 100 mM sucrose in zone Z3 of the primary axis. Bar represent the mean number of outgrowing buds over each zone 20 days after FBV (*n*=15, 20, 9, 15 for *A*, *B*, *C*, *D*, respectively). Asterisks indicate significant difference between bud outgrowth rates of controlled and treated plants (Fisher's exact test; *: $p<0.05$; ***: $p <0.001$).

Figure 9. Schematic diagram of the effect of light treatment on the source–sink balance within the plant. Compared to plants submitted to continuous high light (HH), plants submitted to continuous low light (LL) have a lower sugar availability due to reduced incident light (Fig. 5B) inducing a lower photosynthesis and carbon (C) supply (Fig. 5D); the development of apical organs is also reduced, inducing a reduction in C demand (Fig. 7B), but this effect was much smaller than the effect on C supply,

explaining the lower sugar availability. Conversely, plants submitted to transient low light (LH)- ending just before the start of bud outgrowth period-, display a higher sugar availability due to a non-reversible reduction of apical organ development (Fig. 6) and thus C demand (Fig. 7B), while C supply by photosynthesis was poorly affected (Fig. 5D).

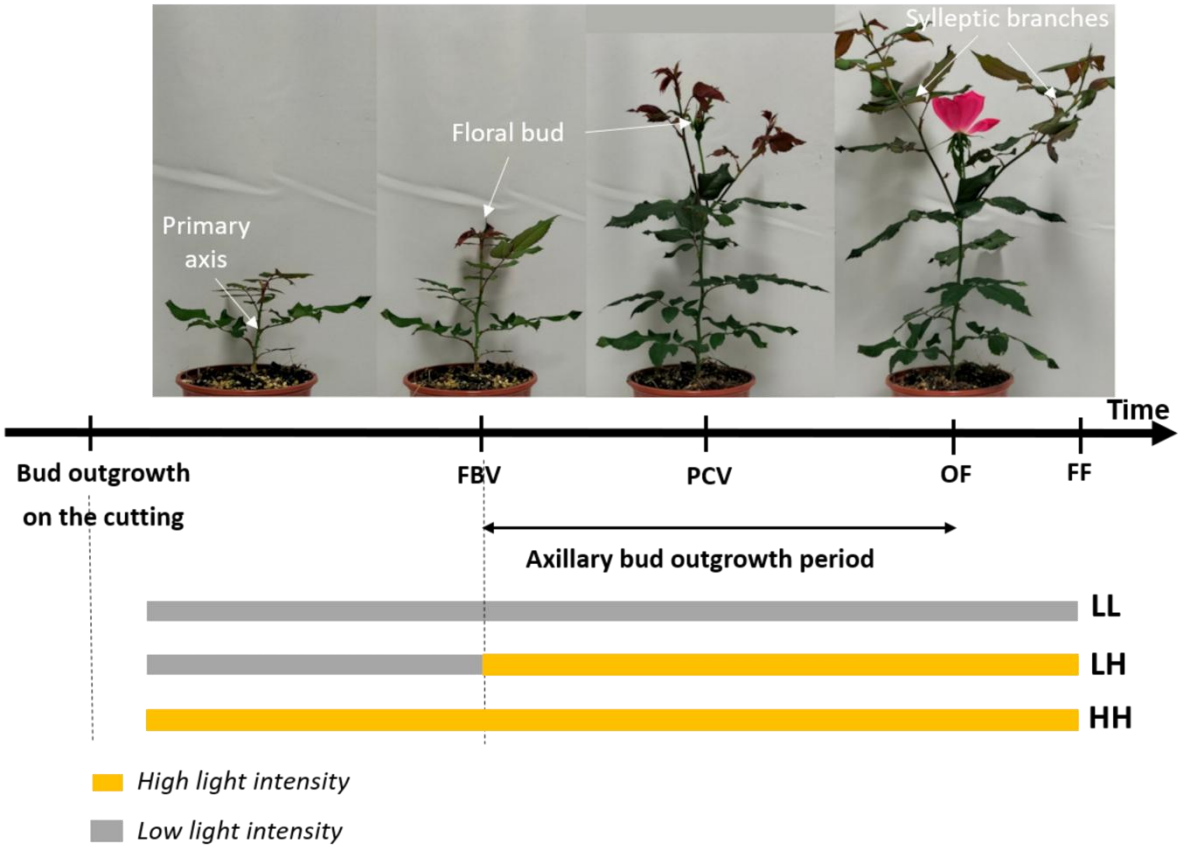

Figure 1. Light treatments applied to rose plants during their development. From plant emergence from a single-node cutting, plants were rapidly transferred to a growth chamber where they were submitted to different regimes of light intensity: (i) LL (Low-Low, grey strip): a constant low light intensity; (ii) HH (High-High, orange strip): a constant high light intensity; (iii) LH (Low-High): a temporary light limitation until the floral bud becomes visible at the top of the primary axis (FBV stage), i.e. before axillary buds started to grow out. *FBV:* floral bud visible; *PCV*: petal color visible; *OF*: opened flower: *FF*: faded flower.

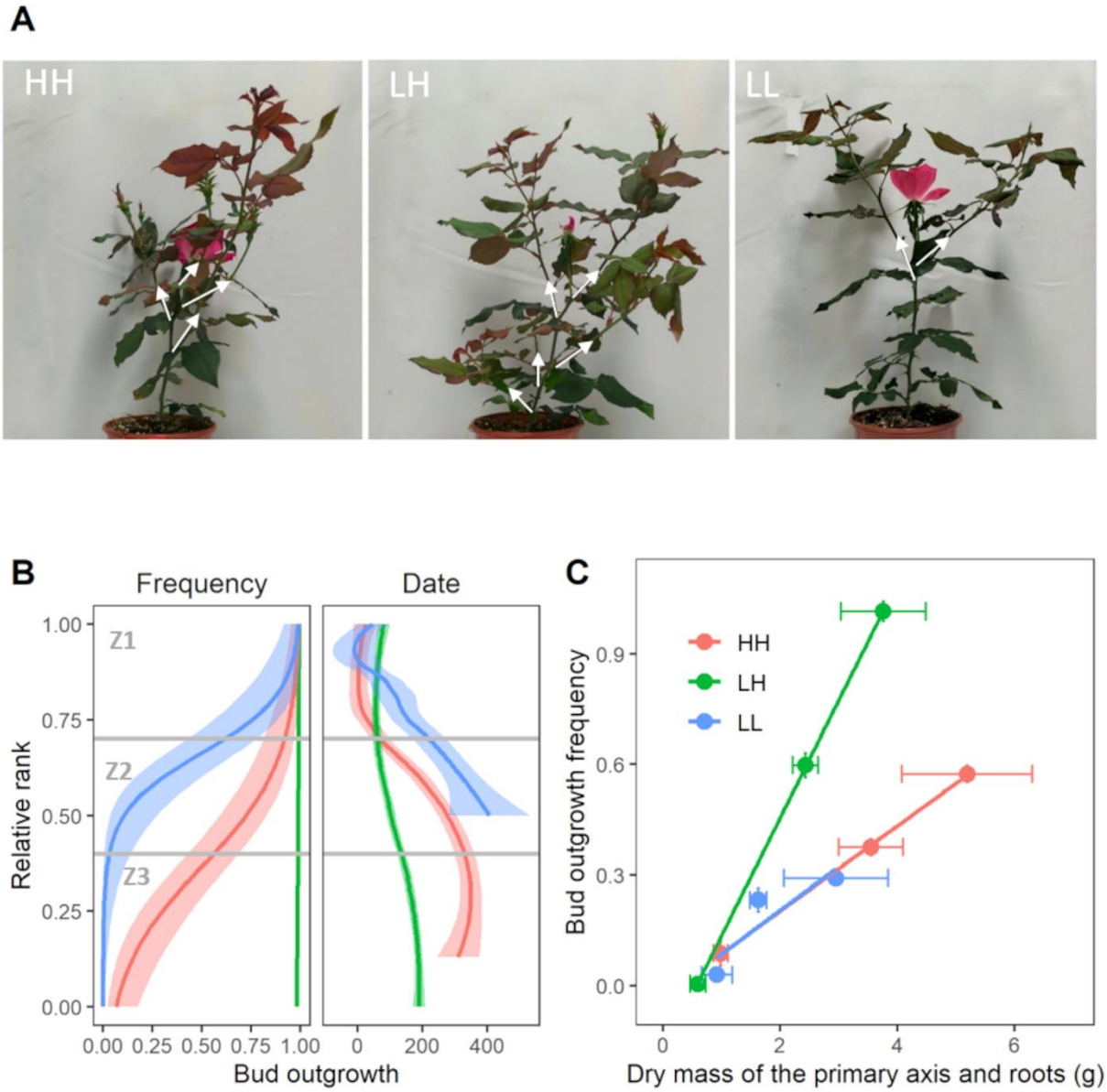

Figure 2. Axillary bud outgrowth was repressed by continuous light limitation but stimulated by transient light limitation compared to continuous high light. (***A***) Pictures of a rose plant at opened or faded flower stage (*OF*). White arrows represent lateral branches. (***B***) Outgrowth frequency and date (expressed as degree days after FBV) for buds at different ranks along the primary axis of rose plants grown under HH (red), LH (green), and LL (blue), in Exp. 1. Rank is expressed relative to the total number of leaves and assigned to a zone (Z1, Z2, Z3; see material and methods). For date, only ranks with a rate > 0.2 are represented. Lines represent logistic and loess smooth lines, respectively, ± 95% confidence intervals (*n*=15 plants for LH and 20 plants for HH, LL). (***C***) Relationship between (i) primary axis and root dry mass and (ii) bud outgrowth frequency for plants grown under HH, LH, and LL. Data are identical to Fig. S3 data. Symbols represent means for each variable, errors bars represent SEM, and lines the estimated linear regression between dry mass and bud outgrowth frequency for each light condition.

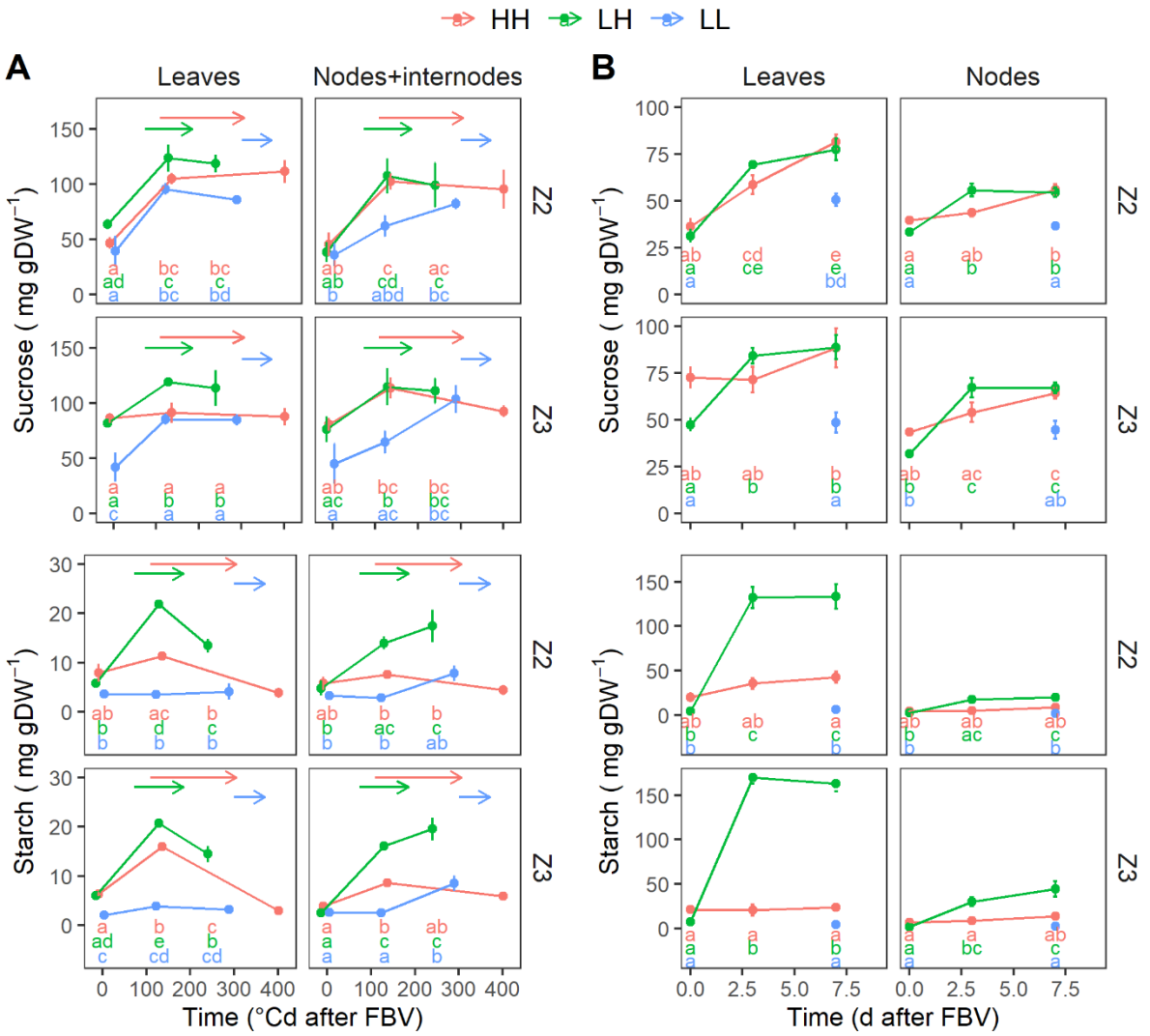

Figure 3. Sucrose and starch levels were reduced after FBV by continuous light limitation but stimulated by transient light limitation. Temporal dynamics of sucrose and starch for zones Z2 and Z3 of rose plants grown under HH (red), LH (green), or LL (blue) in Exp. 1 (***A***) and Exp. 2 (***B***). In (*A*), sugars were quantified in the leaves or internodes+nodes of each zone all over primary axis growth, including bud outgrowth period; horizontal arrows indicate bud outgrowth period, with the start of the arrow being the date at which bud outgrowth starts in Z2. Data are means ± SEM (*n*=4-5 plants). Time is expressed in degree days to account for the slight difference in temperature between the two growth chambers where low and high PPFD were applied, respectively. In (*B*), sugars were quantified in the leaves or nodes of each zone, specifically before the beginning of bud outgrowth. Data are means ± SEM of 4 repetitions of at least four pooled plants each. Time is expressed in days. For (*A*,*B*), different letters indicate significant differences between treatments and sampling dates (ANOVA followed by a Tukey test, $p < 0.05$). In (*B*), no measurement was made for LL plants at time=0 considering an identical value to LH plants (shifted to high light just after time 0; blue letter written but identical to the green letter).

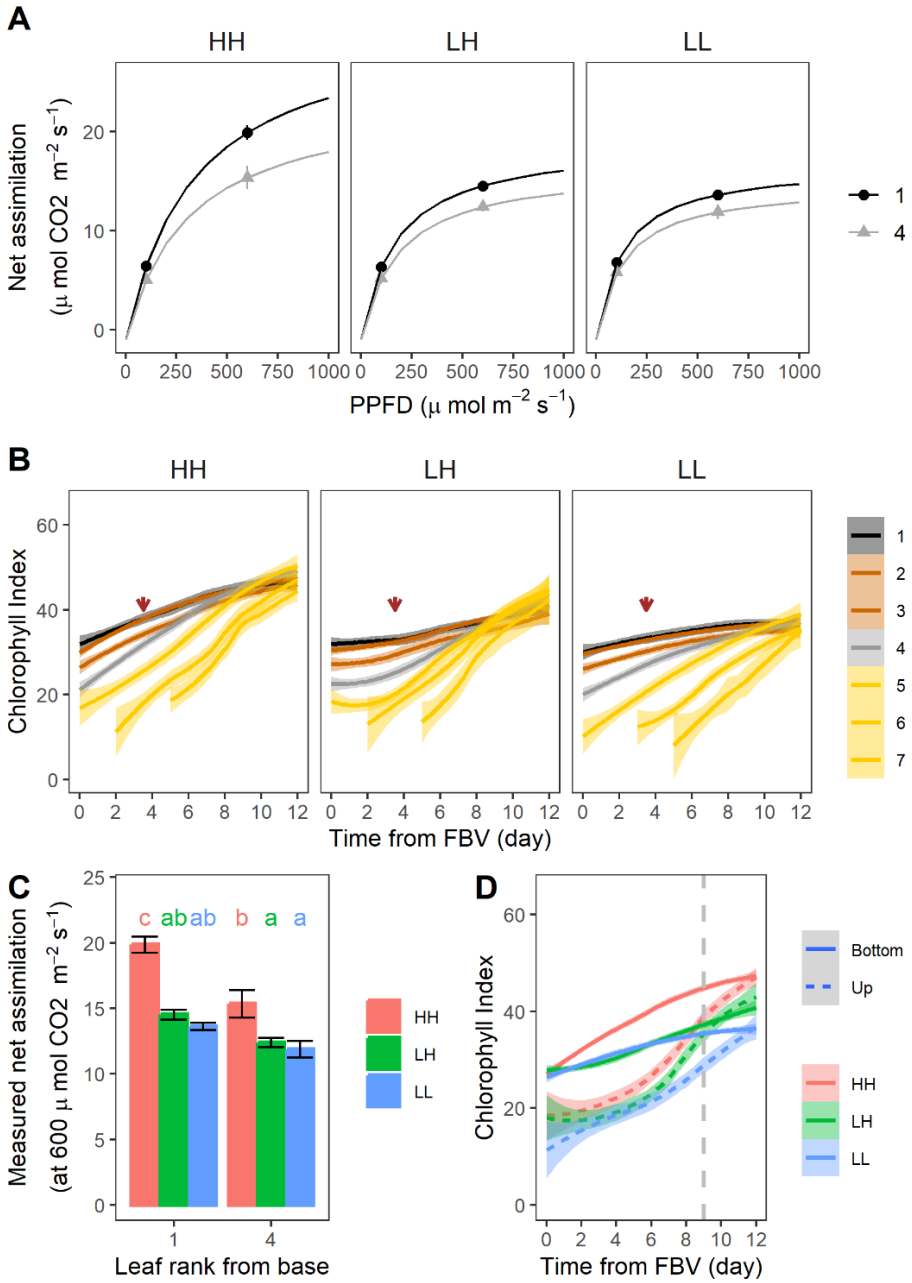

Figure 4. Leaf photosynthesis capacity was reduced after FBV for continuous and temporary light limitation. (***A***) Measured (symbols) and fitted (lines) CO_2 net assimilation of mature leaves 1 (black) and 4 (grey), counting from base, of rose primary axes grown under HH, LH, or LL in Exp. 3. Measurements were made 3 or 4 days after FBV at a PPFD at leaf level of 100 or 600 µmol m^{-2} s^{-1}, and are means ± SEM of 5 plants. Asterisks indicate significant differences between leaf ranks at each PPFD level (Student's test, p<0.05). Estimations were made by fitting a rectangular hyperbola (Equation 5). (***B***) Measured chlorophyll index as a function of time from FBV for each leaf rank (each line). Data represent loess regressions ± 95% confidence intervals (*n*=15-17 leaves). The brown vertical arrow represents the date at which net assimilation was measured in (*A*). (***C***) Focus on the measured net assimilation at 600 µmol m^{-2} s^{-1} of (A). Different letters indicate a significant difference between ranks and light treatments (pairwise comparison using Tukey test; *P*<0.05). (***D***) Overall chlorophyll index dynamics for the lower fully-expanded leaves (ranks <=4) and the upper expanding ones (ranks >4; *D*; Fig. S5). Data represent loess regressions ± 95% confidence intervals (*n*=45-68 leaves). The vertical dashed grey line represents the date at which bud outgrowth started.

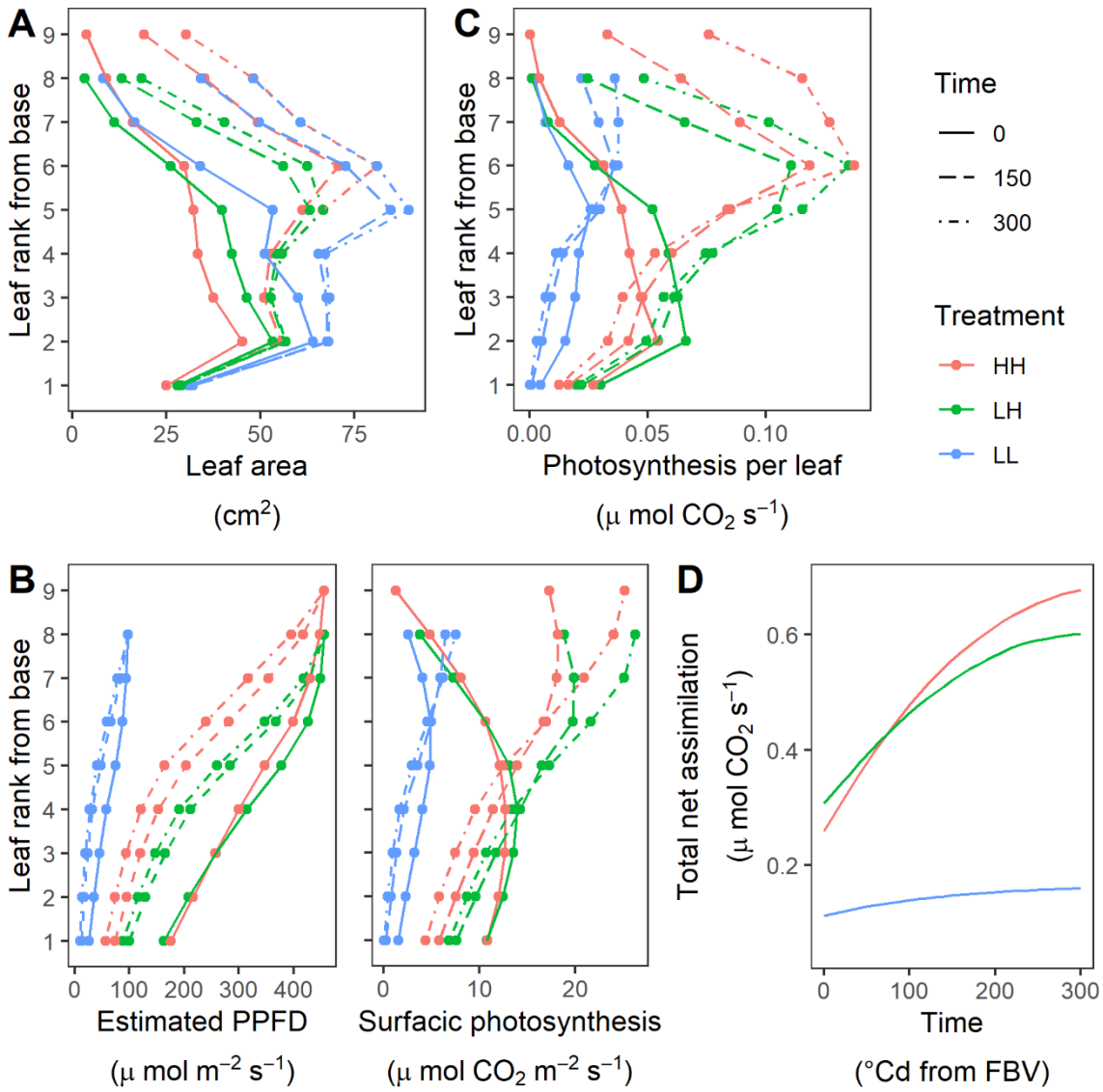

Figure 5. Estimated photosynthesis at primary axis scale was reduced by continuous but not temporary light limitation. Estimated temporal dynamics - between 0 and 300 °Cd - of the photosynthesis determinants and of photosynthesis of primary axes of rose plants grown under HH, LH, or LL in Exp. 1. (***A***) Leaf areas, (***B***) local PPFD and surfacic photosynthesis, (***C***) absolute photosynthesis of individual leaves along the primary axis at 0, 150, and 300 °Cd, and (***D***) photosynthesis of the primary axis through time. Methods for estimations are detailed in material and methods. The estimated primary axes had 9, 8, 8 leaves for HH, LH, LL, respectively, according to the median total number of leaves in each light treatment.

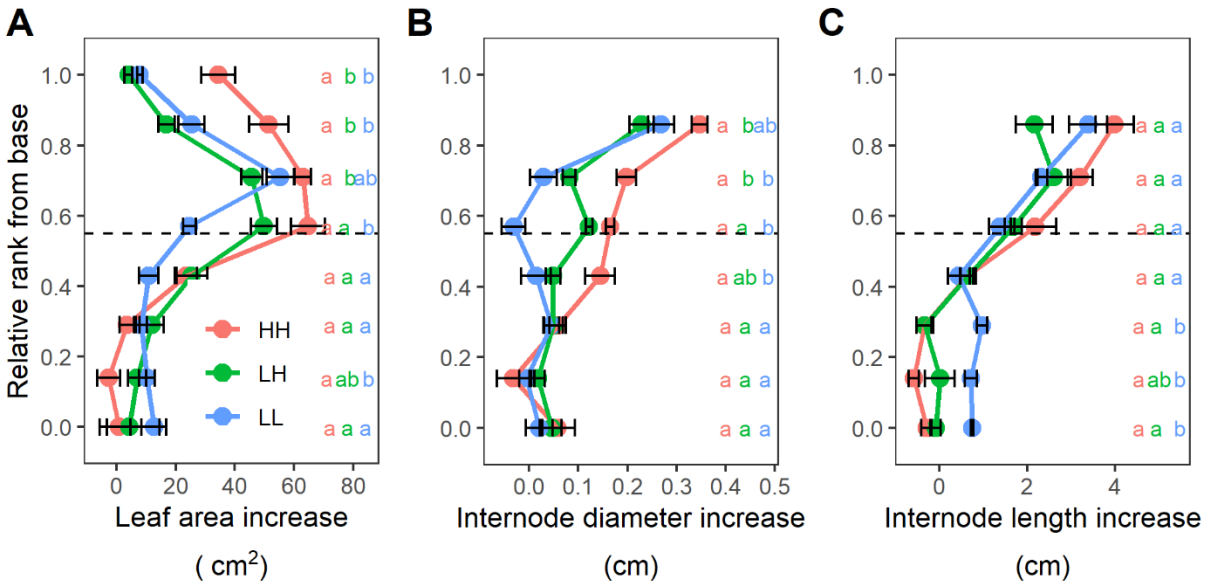

Figure 6. Low light, either continuously or transiently applied, reduced the increase in dimensions of primary axis organs after FBV. Increase - between FBV stage and FBV + *ca.* 130 °Cd - in the leaf area (***A***), the internode diameter (***B***), and the internode length (***C***) according to organ relative rank, for rose primary axes grown under HH, LH, or LL in Exp. 1. The period between FBV stage and FBV + *ca.* 130 °Cd was characterized by sugar accumulation in HH, LH. The horizontal dashed line separates the upper expanding organs to the bottom fully-expanded ones. For each treatment, organs were pooled in 8 groups according to their relative position (see M&M) from plant base. For each group, data are the mean ± SEM of the differences between values at FBV + *ca.* 130 °Cd and the mean value at FBV (*n*= 4-5 plants). Different letters indicate significant differences between treatments (ANOVA followed by a Tukey test, $p < 0.05$).

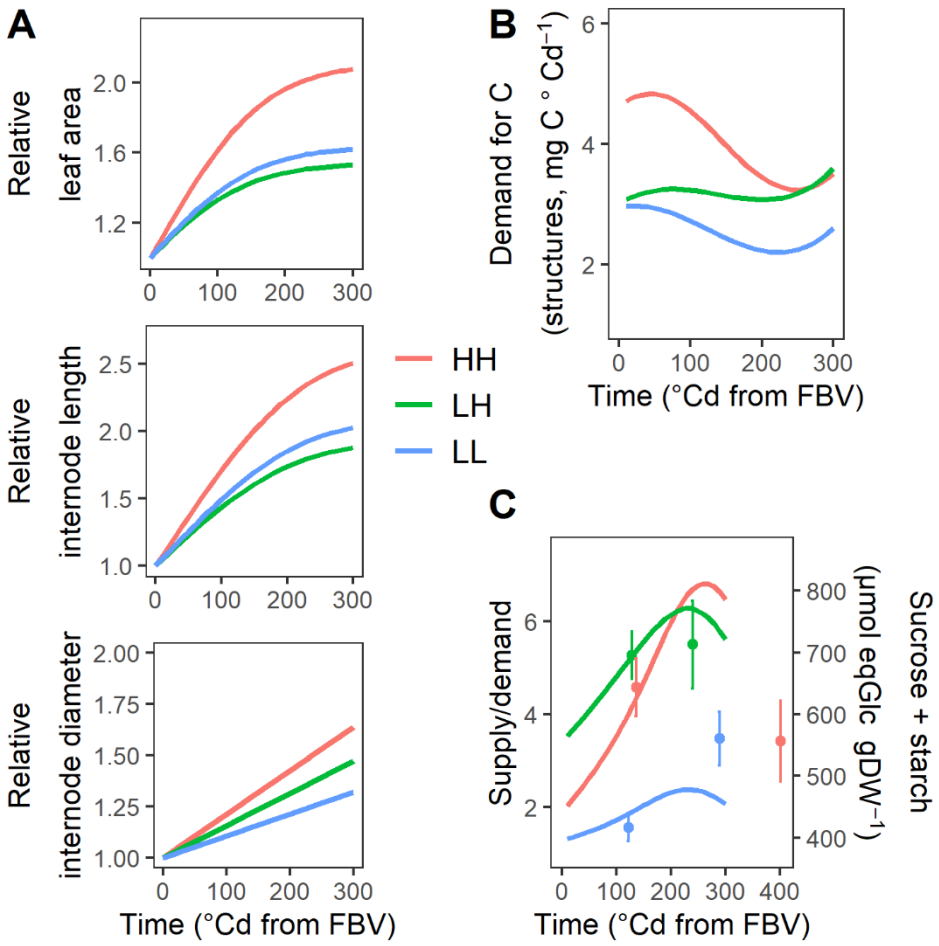

Figure 7. Continuous and temporary light limitation reduced C demand after FBV, and respectively repressed and stimulated C supply-demand balance just after FBV. (***A***) Estimated temporal dynamics - from FBV till 300 °Cd - of components for structural mass estimation of primary axes of Exp. 1 rose plants under HH, LH, or LL: leaf areas, internode/peduncle lengths and diameters. Data on individual organs were cumulated and expressed relatively to values at 0°Cd for lisibility. Estimations for individual organs are presented Fig. S10 to S14. (***B***) Derived estimated temporal dynamics of C demand. (***C***) Derived supply-demand ratio and measured sucrose+starch internode contents (Z2+Z3). Sugar values were means ± SEM (*n*=4-5 plants; data similar to Fig. 3). Methods for estimations are detailed in material and methods. The simulated primary axes had 9, 8, 8 leaves for HH, LH, LL, respectively, according to the median total number of leaves in each light treatment.

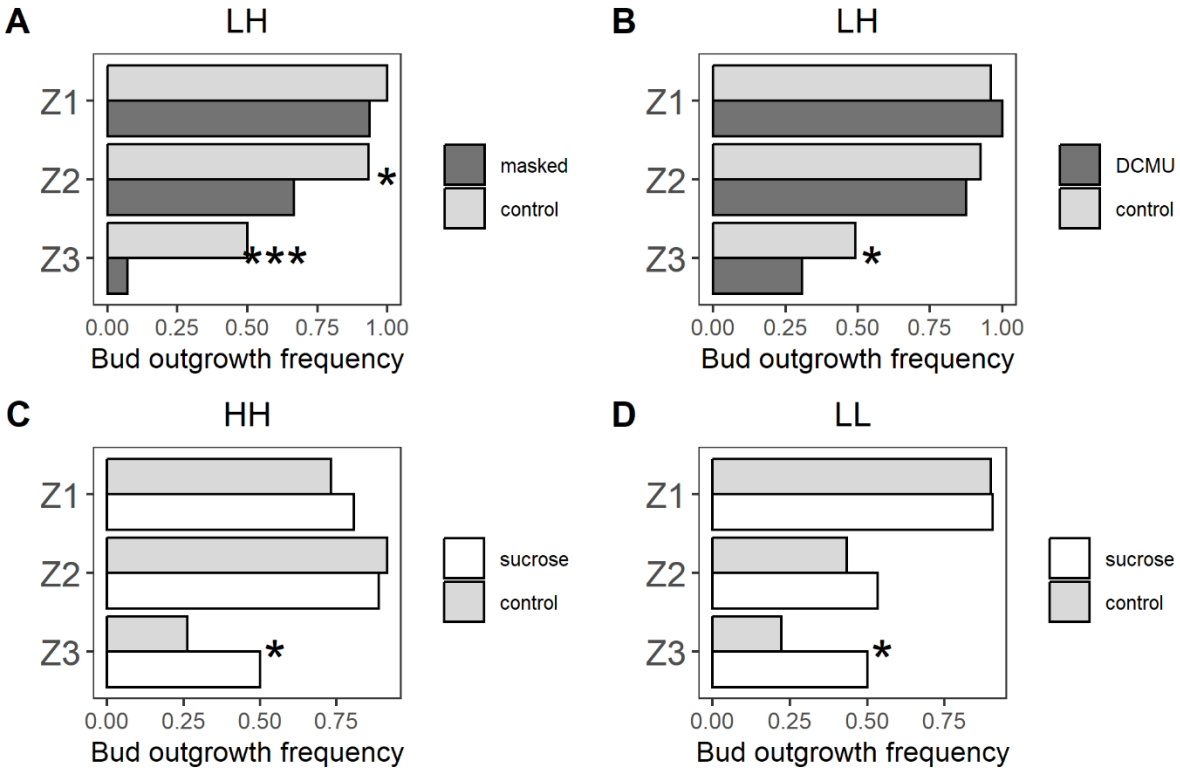

Figure 8. Changes of C supply induced disruptions in bud outgrowth response to light. (***A***, ***B***) Bud outgrowth rate in the three zones along rose primary axes grown under LH with photosynthesis either not decreased (control) or decreased: (*A*) by covering fully opened leaves with either a black plastic (masked) or a transparent film (control) (*B*) or by applying 100 µM DCMU. (***C***,***D***) Bud outgrowth rate in the three zones along rose primary axes grown under HH (*C*) or LL (*D*) and supplied with either 50 mM mannitol (control) or 100 mM sucrose in zone Z3 of the primary axis. Bar represent the mean number of outgrowing buds over each zone 20 days after FBV (n=15, 20, 9, 15 for *A*, *B*, *C*, *D*, respectively). Asterisks indicate significant difference between bud outgrowth rates of controlled and treated plants (Fisher's exact test; *: p<0.05; ***: p <0.001).

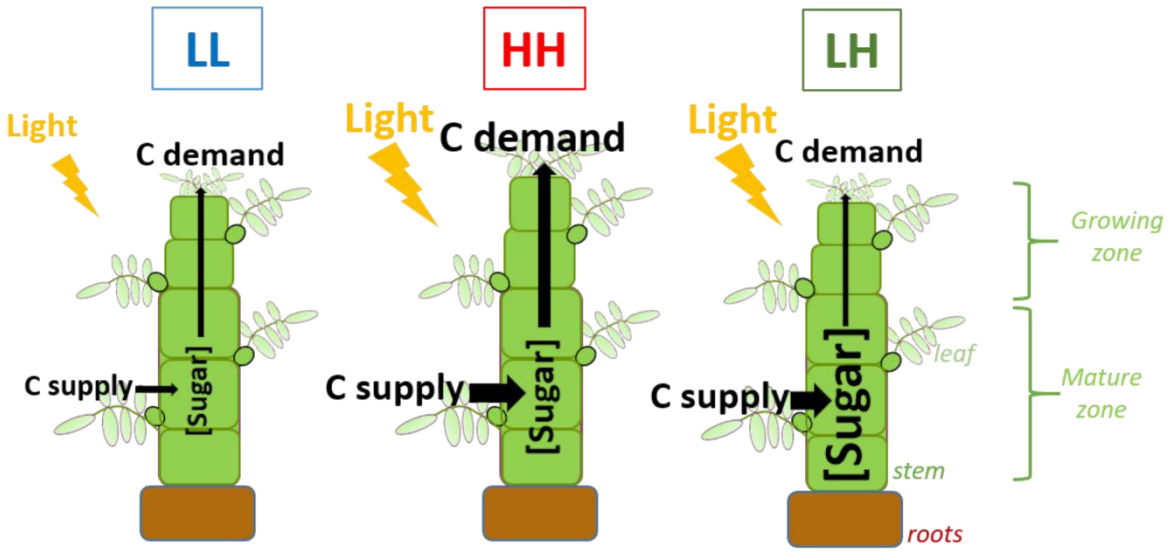

Figure 9. Schematic diagram of the effect of light treatment on the source–sink balance within the plant. Compared to plants submitted to continuous high light (HH), plants submitted to continuous low light (LL) have a lower sugar availability due to reduced incident light (Fig. 5B) inducing a lower photosynthesis and carbon (C) supply (Fig. 5D); the development of apical organs is also reduced, inducing a reduction in C demand (Fig. 7B), but this effect was much smaller than the effect on C supply, explaining the lower sugar availability. Conversely, plants submitted to transient low light (LH)- ending just before the start of bud outgrowth period-, display a higher sugar availability due to a non-reversible reduction of apical organ development (Fig. 6) and thus C demand (Fig. 7B), while C supply by photosynthesis was poorly affected (Fig. 5D).